An increase in surface hydrophobicity mediates chaperone activity in N-chlorinated proteins

Marharyta Varatnitskaya[1], Julia Fasel[1], Alexandra Müller[1], Natalie Lupilov[1], Yunlong Shi[2], Kristin Fuchs[3,4], Marco Krewing[5], Christoph Jung[6,7], Timo Jakob[6,7,8], Barbara Sitek[3,4], Julia E. Bandow[5], Kate S. Carroll[2], Eckhard Hoffmann[9], Lars I. Leichert[1]

[1] Ruhr University Bochum, Institute of Biochemistry and Pathobiochemistry – Microbial Biochemistry, Bochum, Germany

[2] The Scripps Research Institute, Department of Chemistry, 130 Scripps Way, Jupiter, FL 33458

[3] Ruhr University Bochum, Medical Proteome Center, Bochum, Germany

[4] Klinik für Anästhesiologie, Intensivmedizin und Schmerztherapie, Universitätsklinikum Knappschaftskrankenhaus Bochum, Bochum, Germany

[5] Ruhr University Bochum, Applied Microbiology, Faculty of Biology and Biotechnology, Bochum, Germany

[6] Helmholtz Institute Ulm – Electrochemical Energy Storage, Basics of Electrochemistry. Ulm, Germany

[7] Karlsruhe Institute of Technology (KIT), P.O. Box 3640, 76021 Karlsruhe, Germany

[8] Institute of Electrochemistry, Ulm University, Albert-Einstein-Allee 47, D-89081 Ulm, Germany

[9] Ruhr University Bochum, X-ray structure analysis of proteins, Bochum, Germany

Running title: N-chlorination sites in RidA from *E. coli*

*To whom correspondence should be addressed:
Lars I. Leichert
Ruhr University Bochum
Institute for Biochemistry and Pathobiochemistry – Microbial Biochemistry
Universitätstrasse 150
44780 Bochum, Germany
E-mail: lars.leichert@ruhr-uni-bochum.de
Phone +49 234 32 24585, Fax +49 234 32 14332

Keywords: N-chlorination, oxidation, oxidative stress, *E. coli*, chaperone

ABSTRACT

Under physiological conditions, *Escherichia coli* RidA is an enamine/imine deaminase, which promotes the release of ammonia from reactive enamine/imine intermediates. However, when modified by hypochlorous acid (HOCl), as produced by the host defense, $RidA_{HOCl}$ turns into a potent chaperone-like holdase that can effectively protect the proteome of *E. coli* during oxidative stress. We previously reported that the activation of RidA's chaperone-like function coincides with the addition of at least seven and up to ten chlorine atoms. These atoms are reversibly added to basic amino acids in $RidA_{HOCl}$ and removal by reducing agents leads to inactivation. Nevertheless, it remains unclear, which residues in particular need to be chlorinated for activation. Here, we employ a combination of LC-MS/MS analysis, a chemo-proteomic approach, and a mutagenesis study to identify residues responsible for RidA's chaperone-like function. Through LC-MS/MS of digested $RidA_{HOCl}$, we obtained direct evidence of the chlorination of one arginine residue (and, coincidentally, two tyrosine residues), while other N-chlorinated residues could not be detected, presumably due to the instability of the modification and its potential interference with a proteolytic digest. Therefore, we established a chemoproteomic approach using 5-(dimethylamino) naphthalene-1-sulfinic acid ($DANSO_2H$) as a probe to label N-chlorinated lysines. Using this probe, we were able to detect the N-chlorination of six additional lysine residues. Moreover, using a mutagenesis study to genetically probe the role of single arginine and lysine residues, we found that the removal of arginines R105 and R128 leads to a substantial reduction of RidAHOCl's chaperone activity. These results, together with structural analysis, confirm that the chaperone activity of RidA is concomitant with the loss of positive charges on the protein surface, leading to an increased overall protein hydrophobicity. Molecular modelling of $RidA_{HOCl}$ and the rational design of a RidA variant that shows chaperone activity even in the absence of HOCl further supports our hypothesis. Our data provide a molecular mechanism for HOCl-mediated chaperone activity found in RidA and a growing number of other HOCl-activated chaperones.

INTRODUCTION

Phagocytosis is a crucial mechanism of our innate immune system used in the defense against and the elimination of pathogens, such as bacteria and fungi. Within the phagosome, a cellular compartment formed from the cytoplasmic membrane during phagocytosis, pathogens are exposed to a complex mixture of different reactive oxygen and nitrogen species, including superoxide radicals, hydrogen peroxide, peroxynitrite, and hypochlorous acid (for comprehensive reviews see Mortaz et al., 2018; Winterbourn et al., 2016).

Hypochlorous acid is produced by the heme enzyme myeloperoxidase from H_2O_2 and chlorine. HOCl is a highly reactive oxidizing and chlorinating agent and one of the most potent oxidants that exist in human cells (Albrich et al., 1981). It is known to cause a variety of modifications in virtually all cellular macromolecules including DNA (Prütz, 1996), lipids (Winterbourn et al., 1992; Carr et al., 1996; Deborde and von Gunten, 2008), carbohydrates (McGowan and Thompson, 1989) and proteins. Amino acid modifications caused by HOCl include oxidation of cysteine and methionine residues and chlorination of tyrosine, lysine, arginine, and histidine (Hawkins et al., 2003; Pattison et al., 2012). Often these modifications are irreversible, leading to protein misfolding and aggregation (Hawkins and Davies, 1999; Winter et al., 2008; Müller et al., 2014), loss of function, and eventual degradation by proteolytic enzymes (Hawkins and Davies, 1999). Thus, modification of proteins by oxidative stressors and HOCl, in particular, is mostly detrimental to their function. However, in some cases, oxidative modifications can also regulate and activate functions of some proteins to help the cell overcome those oxidative stress conditions. Long-established among the oxidative modifications that can lead to protein activation are reversible oxidations of the side chain of cysteines. Prime examples are transcription factors such as OxyR (Storz et al., 1990; Zheng et al., 1998) or the redox-regulated chaperone Hsp33 (Jakob et al., 1999) in *E. coli*. Both proteins become activated upon the formation of disulfide bonds and, conversely,

reduction of these disulfides leads to their inactivation. More recently we discovered that N-chlorination of basic amino acid side chains, such as lysine and arginine, is another *in vivo*-reversible modification that mediates the activation of a chaperone-like holdase function in the bacterial protein RidA. After treatment with HOCl or monochloramine, we observed an approximately 60 % reduction in the amino group content accompanied by an increase in RidA's hydrophobicity. Consistent with this finding, mass spectrometry (MS) analysis revealed the presence of multiple chlorinated species (Müller et al., 2014). This activation of RidA is independent of the oxidation status of its sole cysteine and is fully reversible by DTT, ascorbic acid, glutathione, and the thioredoxin system.

Other proteins, like the bacterial protein CnoX have been found to use a similar mechanism. After activation with HOCl, CnoX, similar to RidA, turns into an effective chaperone-like holdase that can bind a variety of substrate proteins and prevent their aggregation (Goemans et al., 2018). Moreover, CnoX has a thioredoxin domain and can protect its substrates from irreversible thiol oxidation by forming mixed disulfides with them (Goemans et al., 2018). But not only bacterial proteins are affected by N-chlorination: recently we discovered that human plasma proteins, such as human serum albumin, are activated by N-chlorination and act not only as chaperones to protect damaged host proteins but can also activate immune cells promoting their production of ROS (Ulfig et al., 2019) and mediating their antigen processing (Ulfig et al., 2021).

In this study, we identified the residues facilitating RidA's HOCl-driven activation mechanism. Our data suggest that chlorination of basic amino acids by HOCl is not a process that targets one or two crucial amino acids that act as the "switch" affecting the whole protein. Instead, the N-chlorination of multiple residues changes the electrostatic potential of the molecular surface of RidA allowing it to interact with unfolded substrate proteins.

RESULTS

Direct identification of chlorinated sites in RidA after treatment with HOCl revealed chlorination of one arginine and two tyrosines

We previously reported that the enamine/imine deaminase RidA from *E. coli* turns into a potent protein holdase upon N-chlorination of its lysine and arginine residues. RidA, modified in this way ($RidA_{HOCl}$), can protect other cellular proteins from unfolding due to chlorine stress. Previous mass spectrometric analysis of undigested HOCl-treated RidA showed that the reversible addition of at least 7 and up to 10 chlorine atoms to amino acid residues is concomitant with chaperone-like holdase activity in this protein (Müller et al., 2014). However, it remains unknown, which residues are modified and which of those are required for activation. If we consider arginine, histidine, and lysine as potential targets for a reversible N-chlorination, RidA has 15 possible N-chlorination sites: 5 arginines, 1 histidine, 8 lysines, and the protein's N-terminus (Figure 1).

```
1    MSKTIATENAPAAIGPYVQGVDLGNMIITSGQIPVNPKTGEVPADVAAQA
51   RQSLDNVKAIVEAAGLKVGDIVKTTVFVKDLNDFATVNATYEAFFTEHNA
101  TFPARSCVEVARLPKDVKIEIEAIAVRR
```

Figure 1. The amino acid sequence of the *E. coli* protein RidA (Uniprot entry number: P0AF93). Lysines (K) are highlighted in pink, arginines (R) in purple, and histidine (H) in blue.

To elucidate which amino acids are affected by chlorination, we first performed a mass spectrometric analysis of N-chlorinated RidA after proteolytic digest, specifically searching for peptides having an added mass due to chlorination. Among the above-mentioned 15 possible N-chlorination sites, we were only able to identify R51 to be chlorinated in any of the three replicates after digest with trypsin (Table 1, Figure 2). The monoisotopic mass of the chlorinated peptide containing R51 was ~ 33.96 Da heavier than the unmodified peptide, corresponding to the monoisotopic mass of a chlorine atom minus the monoisotopic mass of the hydrogen atom it replaced. The same tell-tale mass difference could be observed in 9 fragment y-ions containing R51 (Figure 2C). Additionally, we found two chlorinated

peptides containing the two tyrosines present in RidA (Y17, Y91) (Table 1). Tyrosine chlorination by HOCl is an irreversible modification that occurs with a much slower rate than the chlorination of lysine, histidine and arginine (Hawkins et al., 2003). But once formed, chlorotyrosine is highly stable (Winterbourn and Kettle, 2000; Hendrikje Buss et al., 2003). Our previous experiments showed that the 7 to 10 added chlorine atoms observed in full-length MS are virtually all removable by DTT, inconsistent with chlorinated tyrosine residues. We thus concluded that our finding is, due to the high stability of the modification in question, probably of auxiliary nature with no functional relevance.

We suspected that the low number of identified N-chlorinated residues in our experiment could be caused by our use of trypsin. Trypsin, the protease most commonly used for the MS analysis of proteins, cleaves proteins after lysine and arginine, the very residues which we suspected to be modified by HOCl. As chlorination of these residues might interfere with trypsin's ability to recognize them, we additionally prepared a digest with chymotrypsin. Nevertheless, we were still not able to detect more N-chlorinated residues in our chymotryptic digest in any replicate but only re-identified chlorinated tyrosines Y17 and Y91 (Table 1).

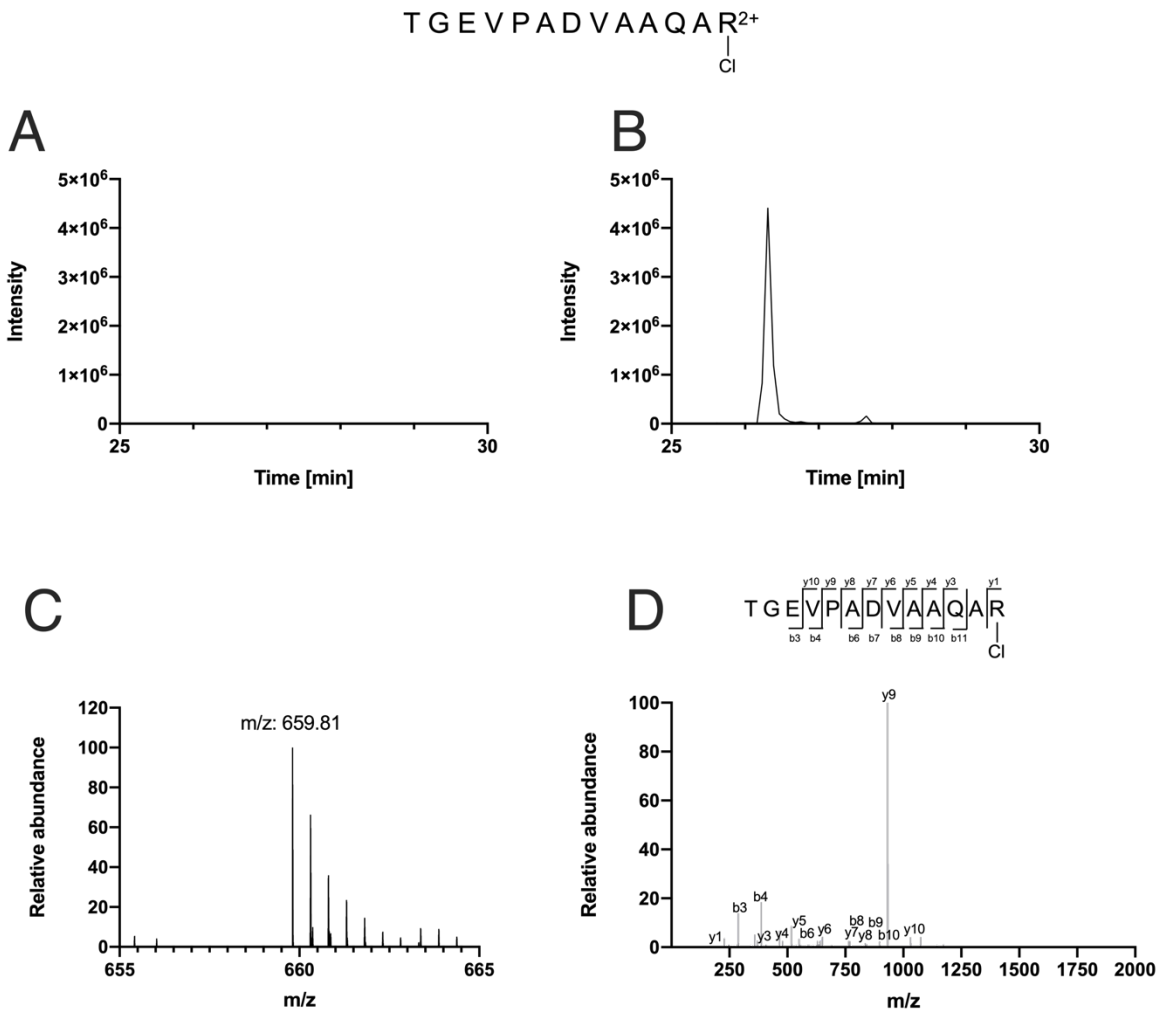

Figure 2. Arginine R51 is chlorinated upon treatment with HOCl. (A, B) Extracted ion chromatograms (XIC) of m/z 659.81, corresponding to the mass of the N-chlorinated peptide TGEVPADVAAQAR$_{51}$ at a retention time from 25 to 30 minutes. A tryptic digest of untreated RidA produces no ion with the respective m/z **(A)**, while RidA treated with a 10-fold molar excess of HOCl shows a peak at 26.265 min **(B)**. **(C)** Primary MS spectrum of the N-chlorinated arginine-containing peptide TGEVPADVAAQAR$_{51}$. **(D)** Corresponding fragment spectrum of the N-chlorinated peptide contains signals corresponding to 9 y-ions containing the chlorine atom.

Table 1. Retention times (RT) and properties of unchlorinated and chlorinated peptides identified by LC-MS/MS after tryptic or chymotryptic digest of HOCl-treated RidA. Methionine sulfoxidation is highlighted in red, and possible sites of chlorination are labeled blue. The PEP-score (posterior error probability) calculated by MaxQuant indicates the probability that a peptide was falsely identified (Käll et al., 2008; Cox and Mann, 2008)

Protease	Residues	Peptide sequence	Unclorinated			Chlorinated		
			m/z, charge	RT, min	PEP-score	m/z, charge	RT, min	PEP-score
Trypsin	4-38	TIATENAPAAIGPY_{Cl}VQGVDL-GNM_{OX}IITSGQIPVNK	1189.29, +3	47.17	8.21×10^{-72}	1200.95, +3	49.29	4.28×10^{-47}
Trypsin	39-51	TGEVPADVAAQAR_{Cl}	642.83, +2	25.88	4.31×10^{-257}	659.81, +2	26.36	1.81×10^{-5}
Trypsin	80-105	TTVFVKDLNDFATVNATY_{Cl}-EAFFTEHNATFPAR	910.12, +4	45.45	5.45×10^{-20}	918.68, +4	48.90	1.62×10^{-6}
Chymotrypsin	2-19	SKTIATENAPAAIGPY_{Cl}	802.42, +2	31.27	8.66×10^{-250}	819.40, +2	32.81	3.73×10^{-222}
Chymotrypsin	78-91	VKDLNDFATVNATY_{Cl}	785.89, +2	39.82	1.24×10^{-290}	802.87, +2	39.10	2.67×10^{-148}

147 *$DANSO_2H$, a novel proteomic probe for N-chlorinated lysine residues in $RidA_{HOCl}$*

148 Our previous results showed that at least seven and up to ten residues become N-chlorinated in RidA,
149 when it is active as a chaperone. Thus, we were dissatisfied with our limited ability to detect N-
150 chlorinated amino acids using mass spectrometry of proteolytic digests of HOCl-treated RidA. This
151 inability might be due to the inherent instability and high reactivity of N-chloramines. Therefore, we
152 devised a way to stably modify N-chlorinated amino acids.

153 To this end we utilized dansyl sulfinic acid (5-(dimethylamino)naphthalene-l-sulfinic acid, $DANSO_2H$),
154 a derivative of the well-characterized reagent dansyl chloride (5-dimethy1amino)naphthalene-1-sulfonyl
155 chloride, DANSCl), which has been used for a long time to derivatize amines, amino acids, and proteins.
156 It reacts with free amino groups and forms stable, highly fluorescent sulfonamides, that can be separated
157 by HPLC and detected by mass spectrometry. In proteins, DANSCl usually reacts only with the free
158 amino group of lysine and the N-terminus (Hsieh and Matthews, 1985) (Figure 3A). Unlike DANSCl,
159 $DANSO_2H$ is not reactive towards unmodified amino groups. Instead, it reacts with monochloramines,
160 forming the same sulfonamide product as the reaction of DANSCl with corresponding unmodified
161 amines (Figure 3C). This provides us with a method for the selective labeling of N-chlorinated lysine
162 residues. $DANSO_2H$ was synthesized from DANSCl by a reaction with sodium sulfite (Scully et al.,
163 1984). The synthesized molecule had a purity of 95 %. The only contamination present was dansyl
164 sulfonic acid ($DANSO_3H$) (Figure S2), which is chemically inert and does react neither with amino
165 groups nor N-chlorinated residues (Scully et al., 1984). The synthesized $DANSO_2H$ was then used to
166 modify $RidA_{HOCl}$. DANSCl was used as a positive control to modify untreated RidA ($RidA_{UT}$), and, as a
167 negative control, $DANSO_2H$ was incubated with $RidA_{UT}$. As expected, after treatment with DANSCl,
168 $RidA_{UT}$ showed the typical fluorescence of dansyl-modified proteins (Figure 3B). The same fluorescence
169 albeit to a lesser extent was observed in $DANSO_2H$-treated $RidA_{HOCl}$ (Figure 3D). The ~30 % lower
170 fluorescence intensity is consistent with our previous finding that only up to 10 out of 15 potential

chlorination sites are chlorinated in fully active $RidA_{HOCl}$. $RidA_{UT}$ treated with $DANSO_2H$ showed virtually no fluorescence, demonstrating the specificity of our probe (Figure 3D).

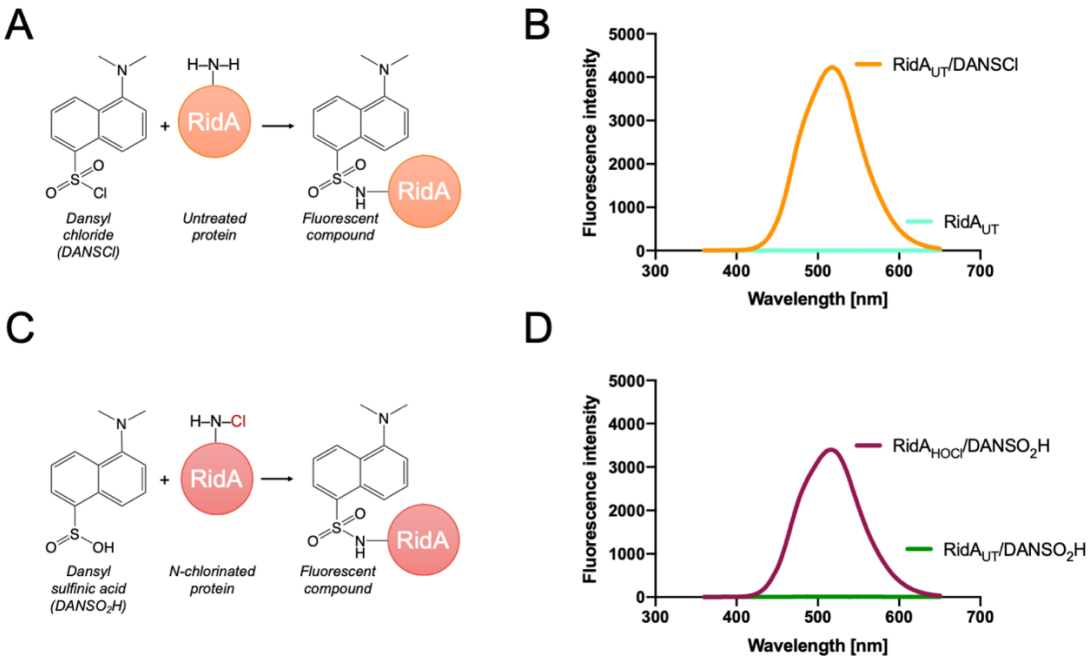

Figure 3. Modification of RidA with dansyl-derived compounds. (A) Dansyl chloride (DANSCl) reacts with an exemplary amino group in RidA forming a "dansylated" fluorescent sulfonamide. **(B)** Dansylation of proteins can be detected using fluorescence spectroscopy at Ex/Em: 340/500 nm. The reaction of $RidA_{UT}$ with a 10-fold molar excess of DANSCl yields a fluorescent protein (orange spectrum), while the protein by itself shows no fluorescence (teal spectrum). **(C)** Dansyl sulfinic acid ($DANSO_2H$) is a derivative of DANSCl and reacts specifically with N-chlorinated amino groups forming the same "dansylated" fluorescent product found in panel (A). **(D)** HOCl-treated RidA ($RidA_{HOCl}$) reacts with a 10-fold molar excess of $DANSO_2H$ producing a fluorescent peak at the expected excitation/emission wavelengths (purple spectrum). Virtually no fluorescent signal was observed with $DANSO_2H$-treated $RidA_{UT}$ (green spectrum).

N-chlorinated lysines can be identified after labeling of $RidA_{HOCl}$ with $DANSO_2H$

Since the fluorescence spectroscopic experiments showed promising results, we then digested the $DANSO_2H$-treated $RidA_{HOCl}$ with chymotrypsin and performed LC-MS/MS analysis. In total, six lysines (K3, K38, K67, K79, K115, K118) were consistently identified as dansylated in all tested samples of $DANSO_2H$-treated $RidA_{HOCl}$ (Table 2). Masses corresponding to these dansylated peptides were not observed in $RidA_{UT}$. Unfortunately, arginines seem not to be modified by $DANSO_2H$, consistent with DANSCl's preference for free amino groups. Dansylated peptides have a mass difference to the

unmodified peptide of ~ 233.05 Da, which equals the mass of $DANSO_2H$ minus the monoisotopic mass of two hydrogen atoms. The dansyl-modification changes the chemical property of a peptide making it more hydrophobic, causing it to elute at significantly higher acetonitrile (ACN) concentrations in the LC. For instance, unmodified peptide harboring K3 eluted at approx. 18 % ACN, whereas the corresponding dansyl-modified peptide eluted at approx. 27 % ACN (Table 2)

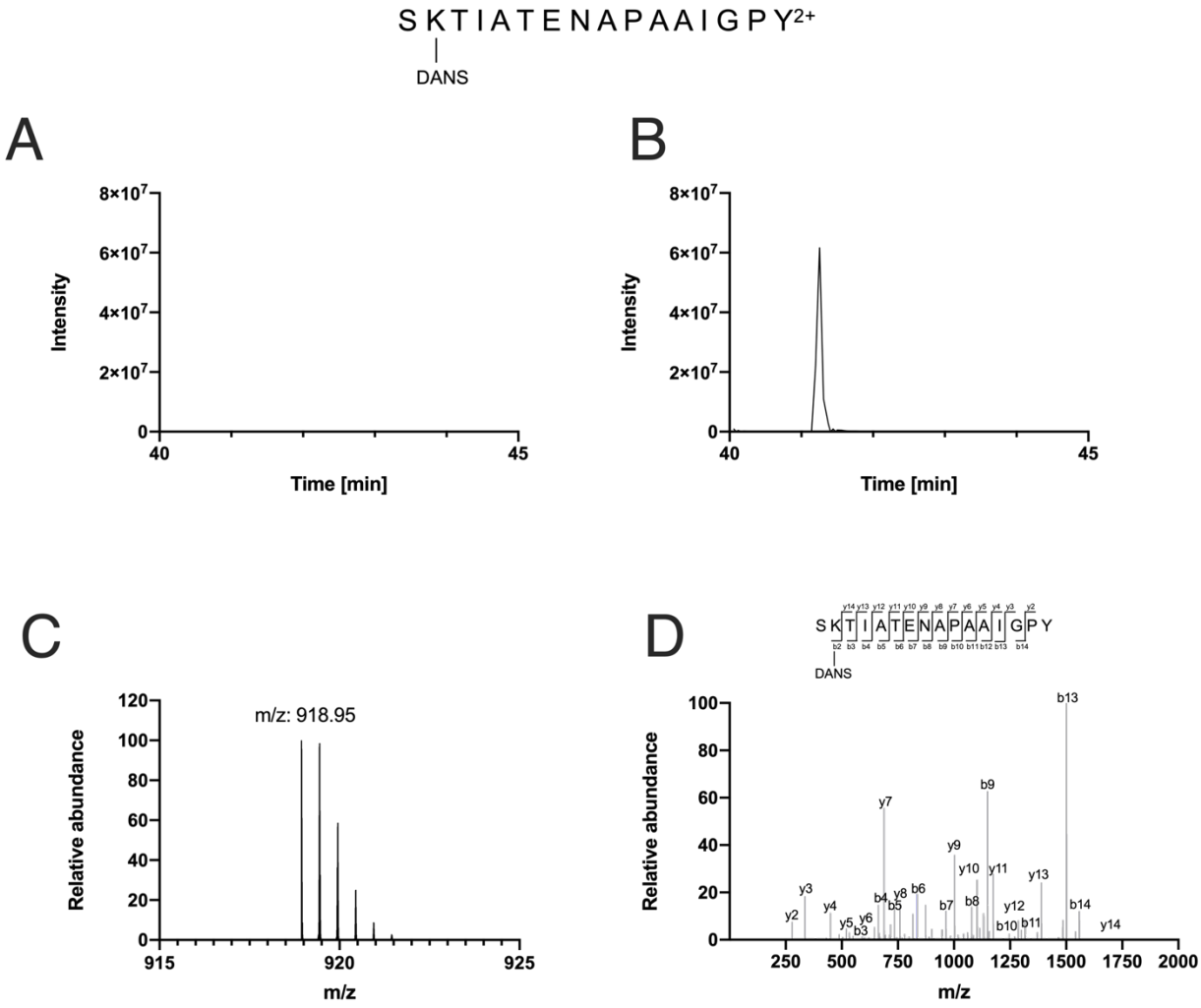

Figure 4. LC-MS/MS analysis of $RidA_{HOCl}$ after treatment with $DANSO_2H$ and subsequent chymotryptic digest. (A, B) Extracted ion chromatogram (XIC) of m/z 918.95, corresponding to the mass of dansylated peptide SK_3TIATENAPAAIGPY at retention times from 40-45 min. **(A)** In the sample derived from $DANSO_2H$-treated $RidA_{UT}$, no ion at this m/z was observed. **(B)** A peak at 41.373 min corresponding to the mass of the dansylated peptide could be observed in $DANSO_2H$-treated $RidA_{HOCl}$. **(C)** Primary MS spectrum of the $DANSO_2H$-modified peptide SK_3TIATENAPAAIGPY found in the digest derived from $DANSO_2H$-treated $RidA_{HOCl}$, at an m/z of 918.95. **(D)** MS/MS analysis revealed that the modified amino acid is lysine K3 at position 2 of the chymotryptic peptide with one y-ion and thirteen b-ions showing the mass shift associated with dansylation.

No dansylated amino acids were found in a $RidA_{UT}$ sample treated with $DANSO_2H$. With this novel chemoproteomic method we were able to gather direct evidence for the N-chlorination of six lysines in the active $RidA_{HOCl}$ chaperone-like holdase.

Mutagenesis reveals two arginines that play an important role in the activation of RidA's chaperone activity

Since $DANSO_2H$ is most likely not suitable for the detection of N-chlorinated arginine residues, we used a mutagenesis approach to test if individual amino acids have a particular impact on the chaperone function of N-chlorinated RidA. We thus engineered a total of 13 RidA variants with every single lysine or arginine residue exchanged to a serine.

These 13 RidA variants were expressed and purified from *E. coli* BL21(DE3) and their chaperone activity after treatment with HOCl was then determined. Activity was tested in a 4-fold excess over citrate synthase. The activity of the variants was compared against wild-type $RidA_{HOCl}$ under the same conditions. The activity of most of HOCl-treated mutants was not affected in a significant way by the exchange of a single N-containing amino acid to serine, when compared to HOCl-treated wild-type protein (Figure 5). However, two variants lacking specific arginines (R105S and R128S) showed a significantly reduced chaperone activity when compared to HOCl-treated wild-type RidA ($RidA_{WT}$).

Table 2. Retention times (RT) and properties of peptides derived from dansyl sulfinic acid ($DANSO_2H$)-labeling of HOCl-treated RidA after chymotryptic digest and LC-MS/MS. Methionine sulfoxidation and cysteine sulfonic acid modifications are highlighted in red, and lysines that are modified with dansyl sulfonic acid are labeled orange. The PEP-score calculated by MaxQuant indicates the probability that a peptide was falsely identified (Käll et al., 2008; Cox and Mann, 2008)

Protease	Residues	Peptide sequence	Undansylated			Dansylated		
			m/z, charge	RT, min	PEP-score	m/z, charge	RT, min	PEP-score
Chymotrypsin	2-19	SK_{DANS}TIATENAPAAIGPY	802.42, +2	28.57	2.24×10^{-250}	918.95, +2	41.37	1.61×10^{-250}
Chymotrypsin	18-54	VQGVDLGNM_{Ox}IITSGQIPVNP-K_{DANS}TGEVPADVAAQARQSL	1263.99, +3	34.61	5.56×10^{-50}	1341.68, +3	41.80	6.63×10^{-38}
Chymotrypsin	67-77	K_{DANS}VGDIVKTTVF	603.86, +2	30.89	5.73×10^{-13}	720.38, +2	41.49	2.26×10^{-8}
Chymotrypsin	78-91	VK_{DANS}DLNDFATVNATY	785.89, +2	33.37	8.66×10^{-136}	902.42, +2	42.05	6.52×10^{-148}
Chymotrypsin	103-128	PARSC_{SO3H}VEVARLPK_{DANS}D-VK_{DANS}EIEAIAVRR	989.56, +3	28.90	1.02×10^{-46}	1144.92, +3	43.91	2.28×10^{-10}

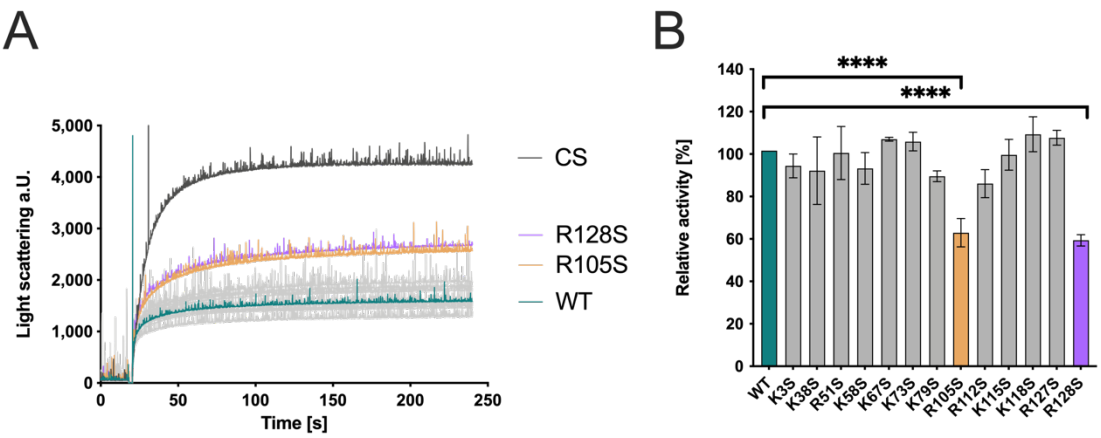

Figure 5. Chaperone activity of RidA variants lacking individual lysine or arginine residues. Chaperone activity was tested in an aggregation assay with citrate synthase. **(A)** HOCl-treated $RidA_{WT}$ (teal) strongly inhibits aggregation of chemically denatured citrate synthase when compared to untreated control (black), as measured by light scattering at 360 nm. All variants, except for R105S (yellow) and R128S (violet), showed activity similar to $RidA_{WT}$. **(B)** Bar graph data represents means and standard deviations from three independent experiments. Differences in chaperone activity of $RidA_{WT}$ between the variants were analyzed using a one-way ANOVA with Tukey's comparison test (****, $p < 0.0001$). The activity of $RidA_{WT}$ was set to 100 %, and all the data are presented in correlation to this control.

The concomitant exchange of R105 and R128 does not further decrease chaperone activity

Since an exchange of arginine 105 or 128 resulted in decreased chaperone activity, a variant harboring both mutations (R105S_R128S) was constructed to investigate if a synergistic effect can be observed. The variants were then also treated with HOCl and used in an 8-fold excess over citrate synthase. However, the chaperone activity of the variant R105S_R128S remained at approximately the same level as the single exchange variants and a further decrease of chaperone activity was not observed (Figure 6).

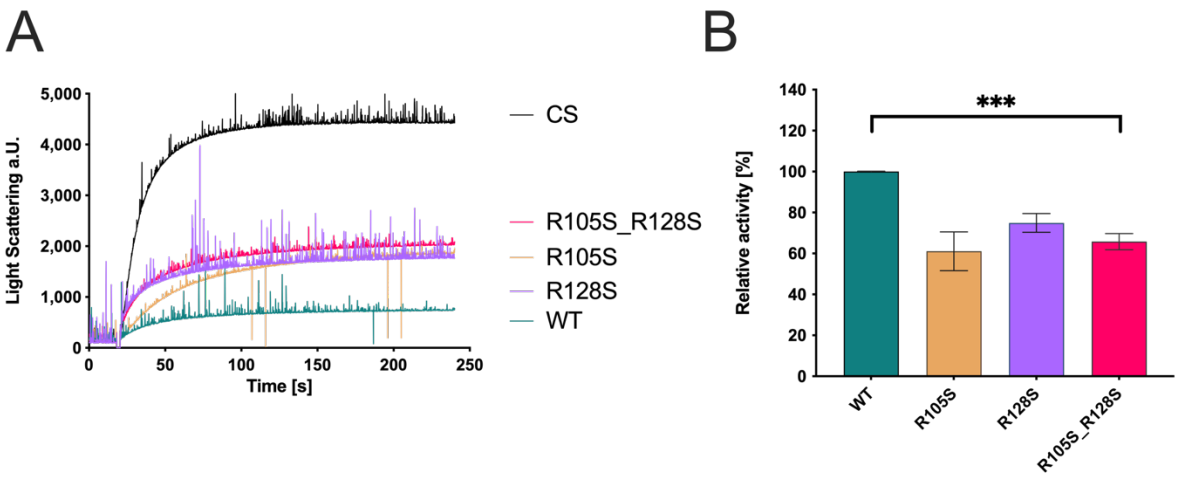

Figure 6. Chaperone activity of RidA double exchange variant R105S_R128S. Chaperone activity was tested in an aggregation assay with citrate synthase. **(A)** HOCl-treated $RidA_{WT}$ (teal) strongly inhibits aggregation of chemically denatured citrate synthase compared to untreated control (black), as measured by light scattering at 360 nm. The concomitant exchange of R105 and R128 against serine (pink) does not further decrease the chaperone activity of RidA and is comparable to single amino acid exchange variants (R105S (yellow) and R128S (violet)). **(B)** Bar graph data represents means and standard deviations from three independent experiments. Differences in chaperone activity between the variants were analyzed using a one-way ANOVA with Tukey's comparison test (***, $p < 0.001$). The activity of $RidA_{WT}$ was set to 100 %, and all the data are presented in correlation to this control.

The activation of RidA's chaperone-like holdase function depends on an overall change of the molecules electrostatic surface.

Summed up, our proteomic, chemo-proteomic and mutagenesis studies suggest that no single amino acid acts as a discrete "switch", but rather the modification of multiple N-containing amino acids leads to the activation of RidA's chaperone-like holdase function. Even arginines 105 and 128, whose individual exchanges to the inert amino acid serine had the largest effect on activatability, did not show synergistic effects when both were removed. Chaperones are known for surface patches that enable them to interact with hydrophobic regions of unfolded proteins. Indeed, our previous experiments showed that $RidA_{HOCl}$ did bind a hydrophobic dye much better than $RidA_{UT}$ (Müller et al., 2014). In order to understand how N-chlorination of basic amino acids changes the surface properties of RidA, we predicted the electrostatic surface potential of RidA, using the known X-Ray structure of RidA (Volz, 2008) (Figure 7A). We then computationally substituted lysine and arginine residues with their chlorinated counterparts within the

structure data set. Using a customized force field, we were then able to predict the electrostatic surface potential of an N-chlorinated RidA molecule as well (Figure 7B). Strikingly, the electrostatic surface potential shifted towards a more negative potential, more or less over the complete surface of the molecule. We thus concluded that the loss of positive electrostatic surface potential is the underlying molecular reason for $RidA_{HOCl}$'s chaperone-like properties.

An engineered variant of RidA mimicking $RidA_{HOCl}$'s surface potential is an active chaperone without HOCl treatment

To test our hypothesis, we decided to engineer a variant of RidA that mimics $RidA_{HOCl}$'s surface potential. To this end, we wanted to mutate all lysine and arginine residues in RidA to more "electroneutral" amino acids. In order to select amino acids that would not lead to a disruption of RidA's structure, we performed a multiple sequence alignment to direct our choice of suitable amino acids. For our mutagenesis, we selected amino acids that occur at the respective position and are mostly uncharged at physiological pH. With the exception of the invariant R105, the arginine in the active deaminase site of RidA, we were able to find a suitable amino acid at all positions. This resulted in a variant, which we termed R0K0_R105 (Figure 8).

The predicted electrostatic surface potential of this R0K0_R105 variant showed a high similarity to the predicted surface potential of N-chlorinated $RidA_{HOCl}$ (Figure 7C).

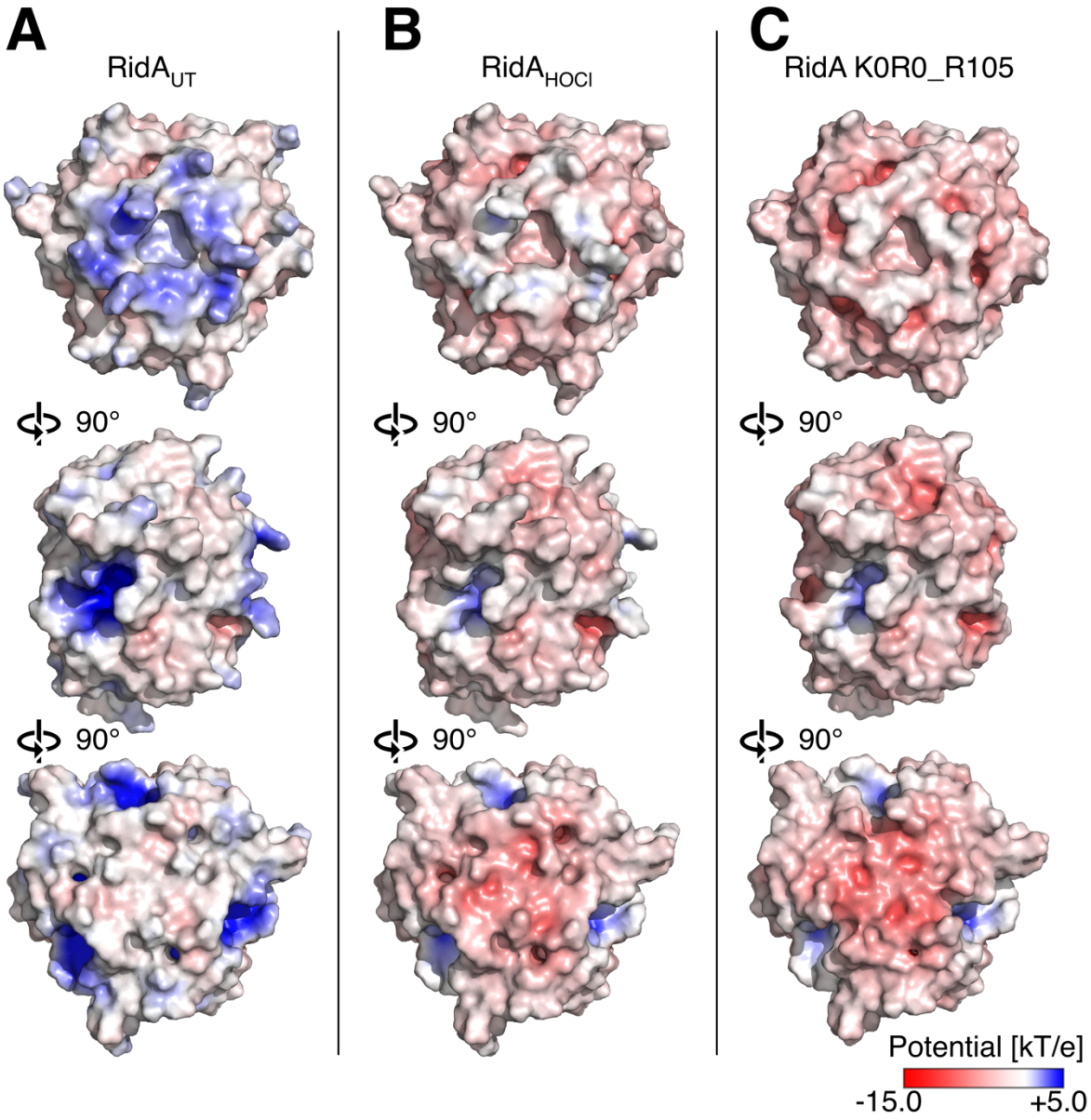

Figure 7. Calculated electrostatic surface potentials of *E. coli* RidA$_{UT}$ (Uniprot entry: P0AF93, PDB entry: 1QU9), RidA$_{HOCl}$, and the K0R0_R105 variant. The C-terminal R128 was added to the RidA structure, as it was only partially resolved in the crystal structure. **(A)** Electrostatic surface visualization of wild-type RidA. The calculation was performed using the Advanced Poisson-Boltzmann Solver in PyMol using the AMBER force field, as described in the materials and methods section. The coloring scale was chosen from -15 to +5 kT/e according to the legend. Middle panel: the molecule rotated 90 degrees around the x-axis in comparison to the upper panel. Lower panel: the molecule was rotated 90 more degrees around the x-axis. **(B)** Electrostatic surface visualization of RidA$_{HOCl}$ using PyMOL. The charge-bearing proton was removed from all lysine and arginine residues, except for R105, and one of the hydrogens was then replaced by a chlorine atom using bond geometries derived from model compounds. The force field (partial charges of respective N and Cl atoms as well as the van der Waals radius of Cl) was adjusted accordingly. **(C)** Electrostatic surface visualization of K0R0_R105. Amino acid exchanges were introduced in RidA's structure using PyMol's "Mutagenesis" function.

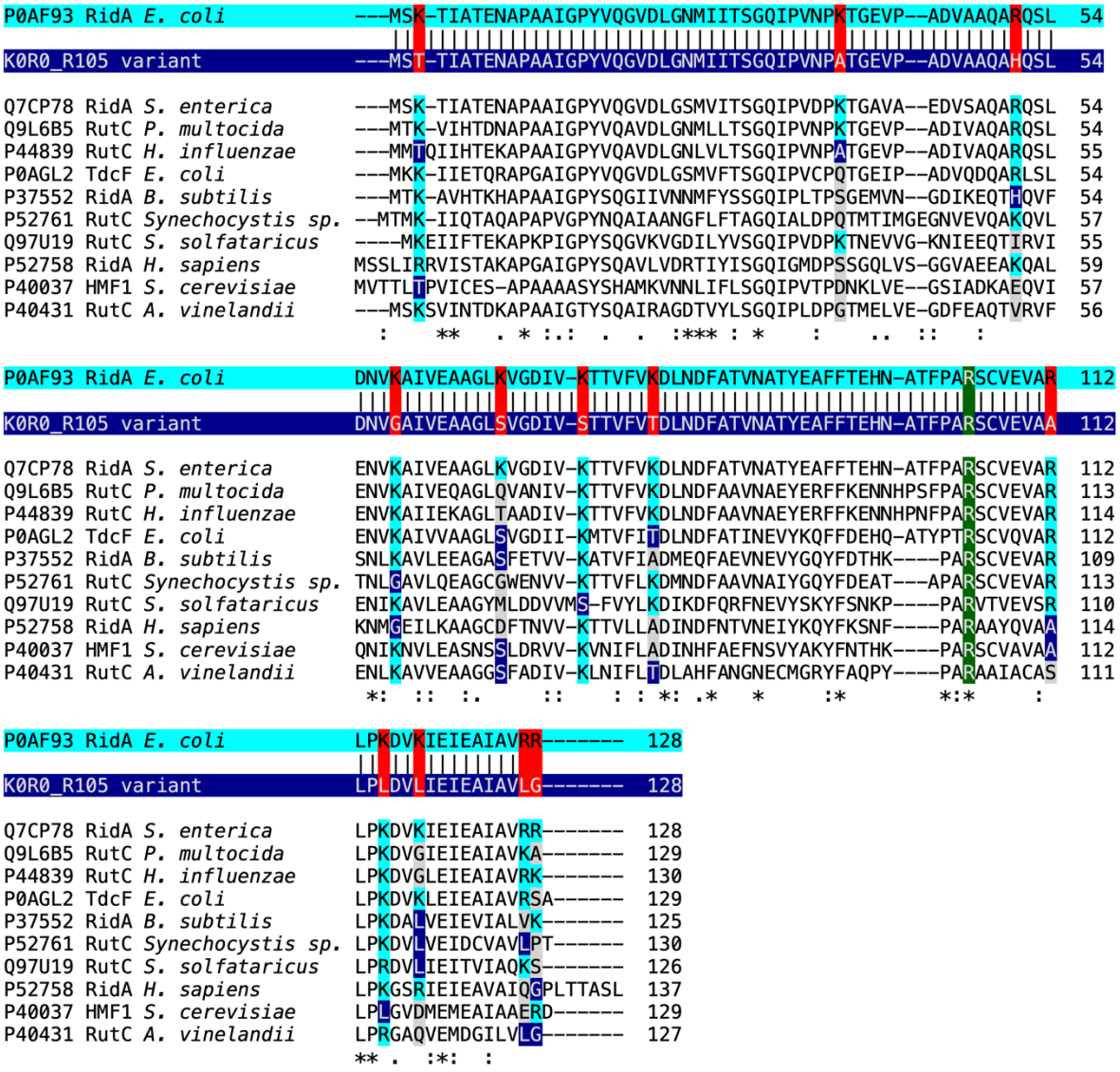

Figure 8. Sequence alignment of wild-type RidA (P0AF93 RidA *E. coli*) with the R0K0_R105 variant and RidA homologs. In the K0R0_R105 variant all lysine and arginine residues were replaced with more electroneutral residues based on amino acids found at those positions in RidA homologs, with the exception of the active-site arginine R105, where no replacement amino acid was found. The order of sequences is based on overall amino acid identity, ranging from 93.75 % *(S. enterica*) to 42.19 % (*A. vinelandii*). Arginine and lysine residues found at the position of the replaced amino acids are highlighted in cyan in the alignment, while amino acids chosen for replacement are highlighted in blue. Other amino acids at those positions are highlighted in grey. The invariant arginine R105 is highlighted in green.

The K0R0_R105 variant was then expressed and purified from *E. coli* BL21(DE3) and its chaperone activity in comparison to $RidA_{UT}$ and $RidA_{HOCl}$ was determined. As predicted, the RidA variant K0R0_R105 showed already potent chaperone-like activity without HOCl pre-treatment, and treatment with HOCl did not increase its chaperone activity significantly (Figure 9). Overall, the activity of K0R0_R105 was indeed comparable to HOCl-treated RidA, supporting our hypothesis.

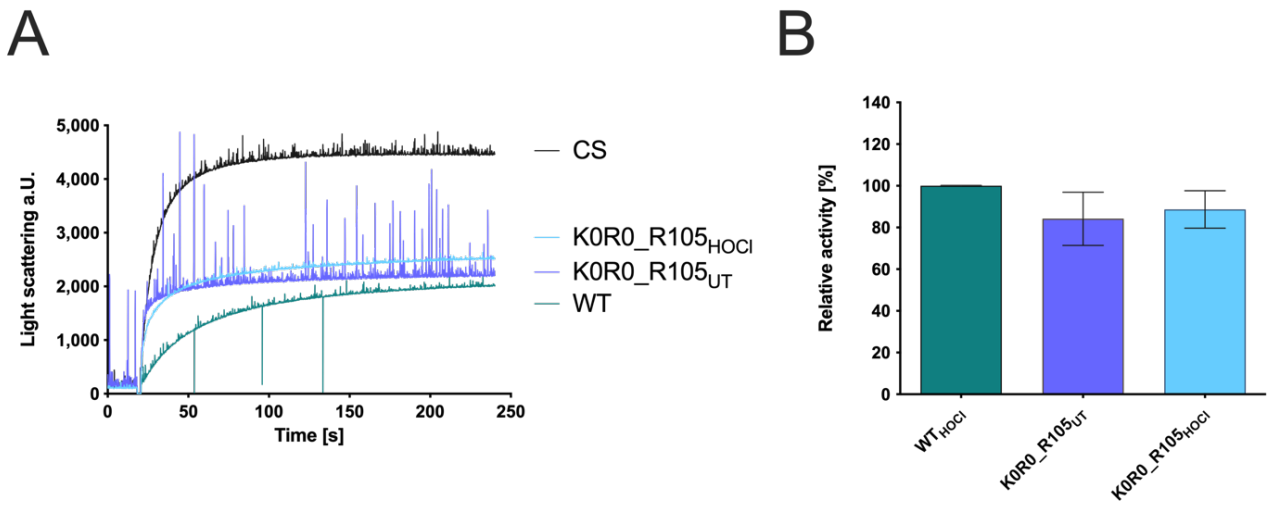

Figure 9. Chaperone activity of the RidA variant K0R0_R105. Chaperone activity was tested in an aggregation assay with citrate synthase. **(A)** HOCl-treated $RidA_{WT}$ (teal) strongly inhibits aggregation of chemically denatured citrate synthase compared to untreated control (black), as measured by light scattering at 360 nm. The variant K0R0_R105 (purple) is fully active as a chaperone without any HOCl treatment, and N-chlorination of this variant (light blue) does not influence its chaperone activity. **(B)** Bar graph data represents means and standard deviations of three independent experiments. Difference in chaperone activity between the untreated and HOCl-treated K0R0_R105 was analyzed using a one-way ANOVA with Tukey's comparison test. The activity of $RidA_{WT}$ was set to 100 %, and all data are presented in correlation to this control.

Taken together, our results suggest that chlorination of basic amino acids by HOCl is not a process that targets one or two crucial amino acids that act as a "switch" that affects the whole protein. Instead, the N-chlorination of multiple residues generates a more negatively charged and hydrophobic molecular surface on RidA, allowing for the interaction with unfolded client proteins. This loss of positive surface charge through N-chlorination is a plausible mechanism for the chaperone-like switch that occurs in a growing number of proteins in response to exposure to HOCl and other reactive chlorine species.

DISCUSSION

After reacting with HOCl or monochloramine, RidA turns into a potent chaperone-like holdase that can bind client proteins. The underlying mechanism was proposed to be the N-chlorination of lysine and arginine residues (Müller et al., 2014). Since then, several other proteins have been discovered that seem to switch to a chaperone-like function upon N-chlorination of basic amino acids. However, it was still unclear if the chlorination of one or several specific residues is decisive for chaperone activity of RidA or rather a general modification of multiple amino acid side chains that affects the overall surface of the protein.

Four proteinogenic amino acids are known to be prone to chlorination (Peskin and Winterbourn, 2001). First, lysines have an amino group on their side chain that can react with HOCl, forming monochloramines. The guanidino group of arginine can also be N-chlorinated. These modifications are thought to be reversed by ascorbate. The side chain of histidine can also react with HOCl, forming a short-lived chloramine. Nevertheless, this chloramine has been shown to be more reactive than corresponding chloramines of lysine and arginine. Moreover, it can rapidly transfer chlorine to other amine groups to generate more stable chloramines (Pattison and Davies, 2005). Additionally, histidines are typically less abundant in proteins in comparison to lysines and arginines. For instance, RidA has only one histidine. Lastly, tyrosine is known to become chlorinated. However, the chlorination of tyrosine is an irreversible reaction and leads to the formation of 3-chlorotyrosine (Hawkins et al., 2003).

LC-MS/MS analysis revealed HOCl-modified arginine, along with two modified tyrosines

Previously our laboratory reported that RidA's full chaperone-like activity is coinciding with the addition of up to 10 chlorine atoms. However, the LC-MS/MS analysis of chlorinated RidA after tryptic digest performed in the current study only revealed one N-chlorinated amino acid, arginine R51. There was also mass spectrometric evidence for the chlorination of both tyrosines present in RidA, but, as mentioned

above, this modification is irreversible and thus should not account for the reversible activation of RidA's chaperone function. Chlorination of lysine or arginine could interfere with the tryptic digest, as these are the amino acids recognized by this particular protease. However, digest with an alternative protease, chymotrypsin did not reveal additional chlorination sites. Alternatively, N-chlorination might potentially be lost during the process of sample preparation, since the amino acid-derived monochloramines, even though less reactive, retain some of the oxidizing capacity of HOCl and are highly reactive towards oxidizable components of reaction buffers (Pattison and Davies, 2006; Ashby et al., 2020). Furthermore, N-chlorinated RidA can potentially react with sulfur-containing amino acids found in the proteases used. Therefore, a direct MS-based identification of chlorinated residues is challenging and does not result in the identification of all modified residues.

Goemans et al. conducted a similar experiment where they performed a mass spectrometric analysis of chlorinated CnoX, in which chaperone activity is also activated by HOCl. Although they identified at least 8 chlorines added to the protein mass during mass spectrometry of full-length CnoX, only five chlorinated amino acid residues were identified using LC-MS/MS analysis after protease digest, among them no lysine residue, hinting at the challenges involved in identifying this particular N-chlorinated amino acid by direct MS analysis (Goemans et al., 2018).

Dansyl sulfinic acid can be used to stably modify N-chlorinated lysines

Searching for ways to chemically label N-chlorinated lysine, and thus making it accessible for MS-based analysis, dansyl sulfinic acid ($DANSO_2H$) caught our attention. It has been previously used to derivatize low molecular weight monochloramines in water and other fluids, allowing for their detection by HPLC (Scully et al., 1984, 1986). We synthesized this probe to label the full-length RidA after its chlorination and found that it exclusively reacts with the HOCl-treated protein. We were able to detect a robust fluorescence signal once N-chlorinated RidA was treated with $DANSO_2H$, but $DANSO_2H$ did not react

with the untreated protein. Therefore, $DANSO_2H$ allowed for the specific labeling of N-chlorinated proteins. Using LC-MS/MS analysis of $DANSO_2H$-derivatized $RidA_{HOCl}$, we identified 6 lysine residues that we were not able to detect using a direct MS-based approach. Interestingly, these 6 lysine residues are also the lysine residues most exposed to the solvent (Table 3), suggesting they are particularly accessible to HOCl.

Table 3. Accessible surface area and accessibility of lysines and arginines of RidA. The analysis was performed using Accessible Surface Area and Accessibility Calculation for Protein (ver. 1.2) (http://cib.cf.ocha.ac.jp/bitool/ASA/). Relative area is the fraction of the amino acid's total area exposed to the solvent.

Amino acid position	Amino acid	Area (Å^2)	Relative area (0.0 – 1.0)
38	LYS	186.596	0.873
67	LYS	150.440	0.704
115	LYS	146.521	0.686
3	LYS	141.010	0.66
127	ARG	103.542	0.451
128	ARG	91.273	0.326
79	LYS	83.866	0.392
51	ARG	81.596	0.356
118	LYS	75.743	0.354
112	ARG	67.246	0.293
58	LYS	52.885	0.247
105	ARG	14.170	0.062
73	LYS	9.844	0.046

$DANSO_2H$ allows for the irreversible derivatization of monochloramines, increasing their stability and simplifying their detection using LC-MS/MS. $DANSO_2H$ initially reacts with monochloramines to form dansyl chloride, which then, in turn, reacts with the newly freed amino group (Scully et al., 1984; Jersey et al., 1990). The specificity of this probe in complex samples might be limited due to this issue, as there is a chance that the dansyl chloride diffuses from the originally modified amino residue. The second order rate constant of the reaction of dansyl chloride and the ε-aminogroup of lysine is 42 M^{-1} $s^{-}1$ (Gray,

384 1967). Therefore, a two-step procedure with blocking of unmodified amino groups might be considered
385 for complex samples prior to labeling with $DANSO_2H$.

386 *Two RidA variants lacking either R105 or R128 showed a significantly decreased chaperone activity*
387 To find out, whether specific amino acids play a key role in the activation of RidA's chaperone-like
388 function, all lysines and arginines were individually changed to serine residues through site-directed
389 mutagenesis. The individual variants were then examined regarding their chaperone activity. The
390 exchange of most lysines and arginines did not affect the chaperone activity of RidA. However, the
391 individual exchange of amino acid residues R105 and R128 resulted in diminished chaperone activity
392 after HOCl treatment. This could indicate that these arginines play a prominent role in chaperone activity.

393 Potentially, these two arginines are particularly accessible to unfolded proteins in N-chlorinated RidA
394 and, therefore, their chlorination might be important for client protein binding. R128 is the C-terminal
395 amino acid of RidA and, based on structural predictions, exposed to the solvent, which makes it
396 especially accessible to unfolded proteins (Table 3). In the bacterial cytoplasm, RidA is present in the
397 form of a trimer (Volz, 2008) and R128, R127, and K3 of every protein subunit form a large positively
398 charged surface patch (visible in the center of the molecule in the upper panel of Fig. 7A), which is
399 predicted to change to a more electroneutral or even negatively-charged patch after N-chlorination (Fig.
400 7 B, upper panel) and thus might allow for binding of unfolded client proteins.

401 The other residue, R105, is highly conserved in three of the seven RidA subfamilies that have
402 enamine/imine deaminase activity (Lambrecht et al., 2012; Liu et al., 2016) and was invariable in all
403 RidA homologs that were identified in a blast search in the SwissProt database (Altschul et al., 1990;
404 Bateman et al., 2021) (see also Fig. 8). In *E. coli* and related species, RidA accelerates the release of
405 ammonia from intermediates that result from the dehydration of threonine by IlvA (threonine
406 dehydratase). Arginine 105 plays a particularly important role in the active center of the protein by

forming a salt bridge with the carboxylic acid of the substrate (Lambrecht et al., 2012). This amino acid is also located in the immediate vicinity of RidA's only cysteine at position 107. This cysteine is redox-sensitive and was modified during the nitrosative stress response (Lindemann et al., 2013). However, the presence of the cysteine is not important for RidA chaperone activity as the mutant lacking the cysteine was as active as wildtype after chlorination (Müller et al., 2014). R105, through its position in the active site, is probably also accessible to client proteins, when N-chlorinated.

We also exchanged both arginines R105 and R128 simultaneously through site-directed mutagenesis. If our argumentation that both arginines are of particular importance for client protein binding were true, we would expect the double mutant to be an even less effective chaperone than the individual mutants. Conversely, the chaperone activity of this variant corresponded approximately to the chaperone activity of the individual exchanges. One explanation would be the distant localization of these two residues, excluding a mutual influence on chaperone-like activity, even if both residues are absent. Alternatively, the lower chaperone-like activity in both single and double mutants might not be due to the lack of an N-chlorination site but the general structural disturbance that an exchange of these residues (especially in the active site of the protein) induces.

The latter possibility is further supported by the fact that the second-order rate constant of the reaction of HOCl with arginines is three orders of magnitude lower than the one for the reaction with lysines ($k = 7.9\times10^3$ $M^{-1}\cdot s^{-1}$ vs. $k = 26$ $M^{-1}\cdot s^{-1}$, respectively) (Pattison and Davies, 2001; Pattison et al., 2012). Hence, lysines are reacting faster with HOCl than arginines. Nevertheless, it is possible that these two residues are particularly reactive with HOCl. Sometimes particular amino acid residues are more reactive than suggested by the reaction rate with model compounds. As such, cysteines are usually oxidized by H_2O_2 with a second-order rate constant of $k=14.7 \pm 0.35$ $M^{-1}s^{-1}$, while certain cysteines in the active site of peroxiredoxins are oxidized at a much higher velocity ($k= 12'000$ $M^{-1}s^{-1}$) (Peskin et al., 2013).

Therefore, it might be that R105 and R128 in RidA are particularly susceptible to N-chlorination due to the microenvironment in the protein's structure.

Electrostatic surface modeling of $RidA_{HOCl}$ and the K0R0_R105S variant revealed the patterns necessary for RidA's chaperone activity

As shown by our MS-based experiments and our mutagenesis studies, N-chlorination affects multiple basic amino acids (at least 9: lysines K3, K38, K67, K79, K115, K118 and arginines R51, R105, R128). Therefore, positive charges on the surface of a protein molecule are eliminated, causing an increase in hydrophobicity, which was previously determined experimentally using Nile Red (Müller et al., 2014; Ulfig et al., 2019) and is demonstrated by the calculated electrostatic surface potential of an N-chlorinated RidA molecule. Protein hydrophobicity as a driving force for chaperone activity is a known mechanism, and other chaperones are also known to have exposed hydrophobic surfaces that allow for the binding of client proteins (Graf et al., 2004; Mayer and Bukau, 2005; Kumar et al., 2005; Koldewey et al., 2016, 2017). A rationally designed variant, which mimics the electrostatic surface potential of N-chlorinated RidA and is indeed constitutively active as a chaperone-like holdase, substantiates this hypothesis.

CONCLUSION

For the activation of the chaperone function of RidA, a significant increase in the protein surface hydrophobicity must take place. We present here computational and experimental evidence that this is achieved by reversible N-chlorination of nine individual lysine and arginine residues. The N-chlorination of these basic amino acids removes positive charges from the surface of RidA allowing it to bind and protect unfolded client proteins in the presence of high HOCl concentrations as they appear during inflammatory processes in bacteria-host interactions.

MATERIALS AND METHODS

Preparation of chlorinating agents

The concentration of NaOCl stock was determined spectrophotometrically using a JASCO V-650 UV/VIS spectrophotometer (JASCO, Tokyo, Japan) at 292 nm using the extinction coefficient ε_{292}= 350 $M^{-1}cm^{-1}$. Monochloramine was prepared freshly by dropwise addition of 200 mM NaOCl solution, dissolved in 0.1 M KOH to 200 mM NH_4Cl solution. After stirring for 5 min, the concentration of the monochloramine produced was measured spectrophotometrically using the extinction coefficient ε_{242} = 429 $M^{-1}cm^{-1}$.

Treatment of RidA with HOCl and monochloramine (MCA)

Chlorination of RidA or RidA variants was achieved by adding 10-fold molar excess of HOCl or MCA to the protein solution. Samples were incubated for 10 min at 30 °C for HOCl-treatment and 45 min at 37 °C for MCA-treatment. Removal of the residual oxidants was achieved by size-exclusion chromatography using "Micro Bio-Spin P30 Tris Chromatography Columns" (Bio-Rad, München, Germany) or Nap-5 columns (GE Healthcare Life Sciences, Amersham, UK) according to the manufacturer's instructions. Final protein concentrations were determined by measuring the absorbance at 280 nm using a JASCO V-650 UV/VIS spectrophotometer with an extinction coefficient of RidA of ε_{280} = 2980 $M^{-1}cm^{-1}$.

Preparation, tryptic and chymotryptic digest of $RidA_{HOCl}$ for mass spectrometry analysis

RidA was treated with HOCl as described above. 5 µl (approx. 25 µg of protein) of untreated and N-chlorinated RidA were mixed together with 35 µl ultrapure water and either 10 µl 5x trypsin digestion buffer (500 mM ammonium bicarbonate, pH 8.0) or 10 µl 5 x chymotrypsin digestion buffer (500 mM Tris-HCl, 10 mM $CaCl_2$, pH 8.0). Freshly reconstituted trypsin in 50 mM acetic acid (1 mg/ml) or chymotrypsin in 1 mM HCl (1 mg/ml) was added to the sample for a final 1:20 enzyme-to-protein ratio.

The sample was digested at 37 °C for 18 h, and afterward, the peptides were purified using OMIX C18 tips. Purified peptides were concentrated to dryness and dissolved in 0.1 % TFA for LC-MS/MS analysis.

Peptide cleanup using OMIX C18 tips

The samples after tryptic or chymotryptic digest were first adjusted to 0.1 % (v/v) TFA using 10 % TFA solution. Then the tips were first equilibrated 2 times with 100 µL 100 % ACN, followed by 2 times washing with 100 µL 50 % ACN, 0.1 % TFA, and lastly 2 times washing with 0.1 % TFA. Afterwards, the sample was loaded onto the tip by pipetting it 8 times slowly up and down without releasing the pipette. The tip was then washed 3 times in 500 µL 0.1 % TFA and the sample was eluted in 40 µL 75 % ACN, 0.1 % TFA by pipetting it 8 times.

Liquid chromatography-mass spectrometry (LC-MS/MS)

Dansyl-derivatized or unmodified peptides after tryptic or chymotryptic digest were analyzed via LC-MS/MS with an LTQ Orbitrap Elite (Thermo Fisher Scientific) as follows: 100 ng of the sample were loaded onto a C18 precolumn (100-µm × 2-mm Acclaim PepMap100, 5 µM, Thermo Fisher Scientific) with 2.5 % ACN/0.1 % TFA (v/v) at a flow rate of 30 µl/min for 7 min. The peptides were then loaded onto the main column (75-µm × 50-cm Acclaim PepMap100 C18, 3 µm, 100-Å, Thermo Fisher Scientific) with 95 % solvent A (0.1 % formic acid (v/v)) and 5 % solvent B (0.1 % formic acid, 84 % ACN (v/v)) at a flow rate of 0.4 µl/min. Peptides were eluted with a linear gradient of 5–40 % B (120 min, 0.4 µl/min). The 20 most intense peaks were selected for MS/MS fragmentation using collision-induced dissociation in the linear ion trap (charge range +2 to +4, exclusion list size: 500, exclusion duration: 35 s, collision energy: 35 eV).

The generated raw files after LC-MS/MS were analyzed using Xcalibur Software (Qual Browser 3.1, Thermo Fischer Scientific, Waltham, MA, USA).

Mass spectrometry data analysis using MaxQuant

MaxQuant software (version 1.5.1.0, DE) was used to identify and quantify dansyl- and chlorine-modified peptides. The following modifications were added to the variable modification list of the search engine Andromeda: dansylation (+233.05, lysine, arginine, and histidine), chlorination (+33.96, lysine, arginine, histidine, tyrosine) and trioxidation (+47.98, cysteine). For peptide search using Andromeda, the *E. coli* K12 proteome database (taxonomy ID83333) obtained from UniProt (4518 proteins, released September 2019, The UniProt Consortium, 2019) was used. Two miscleavages were allowed, Oxidation (M), Dansylation (KR), Chlorination (KRYH), Carbamidomethyl (C), Trioxidation (C) were chosen as variable modification. Identified peptides were assessed using the "peptides.txt" MaxQuant output file. The availability of modification was monitored using "dansylation-sites.txt", "chlorination-sites.txt" and "modificationSpecificPeptides.txt" output files. Data was imported and analyzed using Microsoft Excel Version 16.20 (Microsoft, Redmond, WA, USA). All peptide modifications were verified by manual examination of MS/MS spectra using the criteria proposed by Nybo et al., 2018. Described criteria are: 1) identification of unmodified peptide; 2) coverage of modification site by fragment ion series; 3) correct assignment of peaks in MS/MS spectra (neutral losses: Met + O (−64), Met + 2O (−80), Cys + O (−50), Cys + 2O (−66), Cys + 3O (−82)); 4) similar fragmentation patterns between modified and unmodified peptide(s).

Construction of RidA variants with single amino acid substitutions

E. coli strains, plasmids, and primers used in this study are listed in table 4. Single nucleotides in the *ridA* gene were exchanged using PCR-based mutagenesis, known as QuickChange PCR. PCR was performed using 150 ng of pUC19_*ridA* or pEX_ridA-K0R0 as a template and 125 ng of each specific primer (Table 5) for every single exchange. 20 µL of the PCR product were digested with 20 U of DpnI at 37 °C for 1 h to eliminate the template plasmid. Subsequently, *E. coli* XL-1 blue cells were transformed with the sample using a standard heat-shock method and plated on LB agar plates supplemented with 100 mg/ml

520 ampicillin. Plasmid DNA was isolated from single colonies, and successful mutagenesis was verified by
521 sequencing. Afterwards, *ridA* gene variants were subcloned into pET22b(+) expression vector via the
522 restriction sites *Nde*I and *Xho*I. The resulting pET22b(+)-based constructs were transformed into *E. coli*
523 BL21(DE3) cells for the subsequent overexpression of RidA variants.

524 **Table 4: Bacterial strains and plasmids used in this study.**

Strain or plasmid	**Relevant genotype or description**	**Source or Reference**
Strains		
E. coli XL1 blue	*rec*A1 *end*A1 *gyr*A96 *thi*-1 *hsd*R17 *sup*E44 *rel*A1 *lac*	Stratagene
E. coli BL21 (DE3)	*fhu*A2 [lon] *omp*T *gal* (λ DE3) [dcm] *ΔhsdS*	
E. coli DH5α	*fhu*A2 *lac(del)U*169 *phoA gln*V44 *Φ80' lacZ(del)*M15 *gyr*A96 *rec*A1 *rel*A1 *end*A1 *thi*-1 *hsd*R17	17
Plasmids		
pUC19	2686 bp, Amp^R	
pUC19_ridA	3083 bp, Amp^R, *ridA*	A. Baumann
pUC19_ridA_K3S	3083 bp, Amp^R, *ridA*_K3S	This work
pUC19_ridA_K38S	3083 bp, Amp^R, ridA_K38S	This work
pUC19_ridA_R51S	3083 bp, Amp^R, *ridA*_R51S	This work
pUC19_ridA_K58S	3083 bp, Amp^R, *ridA*_K58S	This work
pUC19_ridA_K67S	3083 bp, Amp^R, *ridA*_K67S	This work
pUC19_ridA_K73S	3083 bp, Amp^R, *ridA*_K73S	This work
pUC19_ridA_K79S	3083 bp, Amp^R, *ridA*_K79S	This work
pUC19_ridA_R105S	3083 bp, Amp^R, *ridA*_R105S	This work
pUC19_ridA_R112S	3083 bp, Amp^R, *ridA*_R112S	This work
pUC19_ridA_K115S	3083 bp, Amp^R, *ridA*_K115S	This work
pUC19_ridA_K118S	3083 bp, Amp^R, *ridA*_K118S	This work
pUC19_ridA_R127S	3083 bp, Amp^R, *ridA*_R127S	This work
pUC19_ridA_R128S	3083 bp, Amp^R, *ridA*_R128S	This work
pET22b	5493 bp, Amp^R, T7-Promotor, HIS_6-Tag	Novagen
pET22b_ridA_K3S	5751 bp, Amp^R , T7-Promotor, HIS_6-Tag, *ridA*_K3S	This work
pET22b_ridA_K38S	5751 bp, Amp^R, T7-Promotor, HIS_6-Tag, *ridA*_K38S	This work
pET22b_ridA_R51S	5751 bp, Amp^R, T7-Promotor, HIS_6-Tag, *ridA*_R51S	This work

pET22b_ridA_K58S	5751 bp, Amp^R, T7-Promotor, HIS_6-Tag, *ridA*_K58S	This work
pET22b_ridA_K67S	5751 bp, Amp^R, T7-Promotor, HIS_6-Tag, *ridA*_K67S	This work
pET22b_ridA_K73S	5751 bp, Amp^R, T7-Promotor, HIS_6-Tag, *ridA*_K73S	This work
pET22b_ridA_K79S	5751 bp, Amp^R, T7-Promotor, HIS_6-Tag, *ridA*_K79S	This work
pET22b_ridA_R105S	5751 bp, Amp^R, T7-Promotor, HIS_6-Tag, *ridA*_R105S	This work
pET22b_ridA_R112S	5751 bp, Amp^R, T7-Promotor, HIS_6-Tag, *ridA*_R112S	This work
pET22b_ridA_K115S	5751 bp, Amp^R, T7-Promotor, HIS_6-Tag, *ridA*_K115S	This work
pET22b_ridA_K118S	5751 bp, Amp^R, T7-Promotor, HIS_6-Tag, *ridA*_K118S	This work
pET22b_ridA_R127S	5751 bp, Amp^R, T7-Promotor, HIS_6-Tag, *ridA*_R127S	This work
pET22b_ridA_R128S	5751 bp, Amp^R, T7-Promotor, HIS_6-Tag, *ridA*_R128S	This work
pUC19_ridA_R105S_R128S	3083 bp, Amp^R, *ridA*_R105S_R128S	This work
pET22b__ridA_R105S_ R128S	5751 bp, Amp^R, *ridA*_R105S_R128S	This work
pEX_ridA_K0R0	2846 bp, Amp^R, *ridA*_K0R0	This work
pEX_ridA_K0R0_R105	2846 bp, Amp^R, *ridA*_K0R0_R105	This work
pYP169	2622 bp, Kan^R, *lacZ*	Y. Pfänder und B. Masepohl, unpublished
pYP169_ridA_K0R0_R105	3019 bp, Kan^R, *lacZ*, *ridA*_K0R0_R105	This work
pET22b_ ridA_K0R0_R105	5751 bp, Amp^R, T7-Promotor, HIS_6-Tag, *ridA*_K0R0_R105	This work

525

526 **Table 5: Primers used in this study**

Primer name	Sequence
K3S_fw	CATATGAGCAGCACTATCGCGACGGAAATGC
K3S_rv	CCGTCGCGATAGTGCTCATATGTATATCTCCTTC
K38S_fw	CCCGGTAAATCCGAGCACGGGCGAAGTACC
K38S_rv	GCCCGTGCTCGGATTTACCGGGATCTGAC
R51S_fw	GCACAGGCAAGCCAGTCGCTGGATAACG
R51S_rv	CGACTGGCTTGCCTGTGCAGCGACGTC
K58S_fw	GGATAACGTAAGCGCGATCGTCGAAGCCGC
K58S_rv	CGACGATCGCGCTTACGTTATCCAGCGACTG
K67S_fw	GGCCTGAGCGTGGGCGACATCGTTAAAACTACCG
K67S_rv	GTCGCCCACGCTCAGGCCAGCGGCTTC
K73S_fw	GGGCGACATCGTTAGCACTACCGTGTTTGTAAAAG
K73S_rv	CGGTAGTGCTAACGATGTCGCCCACTTTCAGG
K79S_fw	CCGTGTTTGTAAGCGATCTGAACGACTTCGC
K79S_rv	GATCGCTTACAAACACGGTAGTTTTAACGATGTCGCC
R105S_fw	CCCGGCAAGCTCTTGCGTTGAAGTTGCCC
R105S_rv	CGCAAGAGCTTGCCGGGAAGGTGGCG
R112S_fw	GTTGCCAGCCTGCCGAAAGACGTGAAG
R112S_rv	CGGCAGGCTGGCAACTTCAACGCAAG
K115S_fw	CGTCTGCCGAGCGACGTGAAGATTGAGATCG
K115S_rv	CTTCACGTCGCTCGGCAGACGGGCAACTTC
K118S_fw	GACGTGAGCATTGAGATCGAAGCGATCGC
K118S_rv	CGATCTCAATGCTCACGTCTTTCGGCAGACG
R127S_fw	CGCTGTTAGCCGCCTCGAGCACCACCAC
R127S_rv	CGAGGCGGCTAACAGCGATCGCTTCGATC
R128S_fw	CGCTGTTCGTAGCCTCGAGCACCACCACC
R128S_rv	GCTCGAGGCTACGAACAGCGATCGCTTCG
K0R0_NdeI_ fw	CCCATATGAGCACCACTATCGCGACGG
K0R0_XhoI_rv	GGCTCGAGGCCCAGAACAGCGATC
R105_fw	CCTTCCCGGCACGTTCTTGCGTTGAAGTTGCCGC
R105_rv	CAAGAACGTGCCGGGAAGGTGGCGTTGTGTTCGG

527 *Overexpression and purification of RidA variants*

528 For overexpression, a single colony of *E. coli* BL21 (DE3) carrying the respective pET22b(+) plasmid
529 was inoculated in 50 mL LB containing 200 mg/L ampicillin and grown overnight at 37 °C, 120 rpm.
530 The next morning, the overnight culture was used to inoculate 5 L of LB medium, supplemented with
531 ampicillin, and incubated at 37 °C and 120 rpm until the OD_{600} reached 0.5-0.6. At this point, protein

532 expression was induced by the addition of 1 mM isopropyl 1-thio-ß-D-galactopyranoside (IPTG) to the
533 culture. After 3 h of incubation at 37 °C, 120 rpm, cells were harvested by centrifugation at 7800 x g and
534 4 °C for 45 min and either stored at -80 °C or directly used for the purification procedure.

535 The resulting cell pellet was washed once with lysis buffer (50 mM sodium phosphate, 300 mM NaCl,
536 10 mM imidazole, pH 8.0) containing 1 ml of EDTA-free protease inhibitor mixture (Roche Applied
537 Science). Cells were disrupted by passing the cell suspension three times through a Constant systems cell
538 disruption system TS benchtop device (Score Group plc, Aberdeenshire, UK) at 1.9 kbar and 4 °C,
539 followed by the addition of PMSF to a final concentration of 1 mM.

540 The cell lysate was centrifuged at 6700 x g, 4 °C for 1 h, and the supernatant was vacuum filtered through
541 a 0.45 µm filter. The filtrate was loaded onto a Ni-NTA affinity column. The column was washed with
542 10 mL washing buffer (50 mM sodium phosphate, 300 mM NaCl, 20 mM imidazole, pH 8.0). For
543 purification of the R0K0_R105 variant, washing buffer was additionally supplemented with 1 M NaCl
544 and 0.1 % SDS. Purified proteins were stored at -80 °C and K0R0_R105 was stored at room temperature.
545 Protein concentrations were determined using a JASCO V-650 spectrophotometer using the extinction
546 coefficient ε_{280}=2,980 $M^{-1}cm^{-1}$.

547 *Protein aggregation assay with citrate synthase*
548 Citrate synthase was chemically denatured in 4.5 M GdnHCl, 40 mM HEPES, pH 7.5 at room
549 temperature overnight. The final concentration of denatured citrate synthase was 12 mM.

550 To monitor initial aggregation of citrate synthase, 20 µl of denatured protein were added to 1580 µl of
551 40 mM HEPES, pH 7.5 to a final concentration of 0.15 µM after 20 s of measurement. To test the
552 chaperone activity, RidA or RidA variants were added prior to the addition of citrate synthase to the
553 buffer at different molar access (0.5-16-fold) over dimeric citrate synthase. The increase in light

554 scattering was monitored for 240 s using a JASCO FP-8500 fluorescence spectrometer equipped with an
555 EHC-813 temperature-controlled sample holder (JASCO, Tokyo, Japan). Measurement parameters were
556 set to 360 nm (Em/Ex), 30 °C, medium sensitivity, slid width 2.5 nm (Em/Ex). Relative chaperone
557 activity of different RidA variants was calculated based on the difference between initial and final light
558 scattering. The chaperone activity of wild-type chlorinated RidA was set to 100 %.

559 *Synthesis of N,N-Dimethyl-1-amino-5-naphtalenesulfinic acid (Dansyl sulfinic acid, DANSO$_2$H)*
560 Dansyl sulfinic acid (DANSO$_2$H) was synthesized from dansyl chloride, as described in Scully et al.,
561 1984 with minor modifications. Dansyl chloride (5 g) was added to a continuously stirred aqueous
562 solution of sodium sulfite (10.7 g in 50 mL) warmed to 70 °C. The reaction temperature was kept at
563 80 °C for 5 h. After the solution was cooled, DANSO$_2$H was precipitated from the product mixture by
564 acidifying the solution to pH 4 with concentrated sulfuric acid. The precipitate was then filtered. The
565 precipitate was then dried in a vacuum desiccator over silica gel. The powder was re-dissolved in a cold,
566 aqueous solution of NaOH (2.8 M). The resulting solution was filtered and titrated to pH 4.0 using
567 sulfuric acid. The resulting DANSO$_2$H was dried again in a vacuum desiccator and stored in the light-
568 protected vial at 4 °C. The purity of the resulting dansyl sulfinic acid (retention time 6.48 min) was
569 confirmed by HPLC (Fig. S1) and was 95 %. The 5 % contamination by a corresponding sulfonic acid
570 (retention time 6.55 min) does not affect the derivatization of chloramines (Scully et al., 1984; Alpmann
571 and Morlock, 2008).

572 *Derivatization of RidA with dansyl sulfinic acid and dansyl chloride*
573 200 mM DANSO$_2$H solution was prepared freshly by dissolving the powder in 200 mM NaHCO3 buffer,
574 pH 9.0, and 10 % (w/w) DANSCl stock solution (370 mM) (abcr, Karlsruhe, Germany) in acetone was
575 directly used.

RidA was chlorinated with HOCl as described above. Using an NAP-5 gel filtration column, residual HOCl was removed, and the buffer was exchanged to 200 mM $NaHCO_3$ buffer, pH 9.0. 250 µM $RidA_{HOCl}$ or $RidA_{UT}$ were incubated with a 50-fold molar excess of DANSCl or $DANSO_2H$ for 1h, 37 °C, 1300 rpm. The derivatizing agent was removed using an NAP-5 gel filtration column. Successful derivatization of RidA by monitoring the fluorescence of the resulting sulfonamide was determined by a fluorescence emission scan from 360–600 nm in a JASCO FP-8500 fluorescence spectrometer with the following parameters: 340 nm excitation, 2.5 nm slit width (Ex/Em) and medium sensitivity.

Preparation and chymotryptic digest of dansylated proteins for mass spectrometry analysis

5 µL (approx. 8 µg of protein) of each dansylated sample prepared above were mixed together with 25 µl ultrapure water and 10 µl 5 x chymotrypsin digestion buffer (500 mM Tris-HCl, 10 mM $CaCl_2$, pH 8.0). pH of the resulting solution was monitored to be around 8.0. Then, DTT was added to the solution to a final concentration of 10 mM and incubated at 60 °C for 45 min. After the sample was cooled to room temperature, 3.5 µL of freshly prepared 500 mM iodoacetamide solution in pure water were added to a final concentration of 20 mM. The sample was incubated at room temperature for 30 min, protected from light. To quench the alkylation reaction, 1 ul of 500 mM DTT was added, and the volume of the solution was adjusted to 50 µl using pure water. Chymotrypsin, reconstituted to a concentration of 1 mg/mL in 1 mM HCl, was then added to the sample for a final 1:20 enzyme-to-protein ratio. The reaction mixture was incubated at 37 °C for 18 h. The sample was then desalted using OMIX C18 tips (Agilent Technologies, USA) according to the manufacturer's instructions. Purified peptides were concentrated to dryness and dissolved in 0.1 % TFA for LC-MS/MS analysis.

Protein structure modification and electrostatic surface modelling of RidA, $RidA_{HOCl}$, and K0R0_R105

E. coli RidA crystal structure was accessed using PDB entry number 1QU9 and visualized using PyMOL 2.3.4 (Schrödinger, New York, NY, USA). This structure was converted to a PQR file using the

PDB2PQR webserver (Jurrus et al., 2018) under an assumed pH of 7.0, using PROPKA to assign protonation and the AMBER forcefield to assign partial charges and atomic volumes to the structure's atoms. Using the resulting PQR file as input, PyMol's APBS plugin was used to calculate the electrostatic surface potential.

To model the N-chlorinated $RidA_{HOCl}$, the PQR file of RidA was manipulated using a custom python script (Supplemental Material S2). This script removes charge bearing protons from specified lysine and arginine residues, rectifies binding angles (in case of deprotonated arginine) and replaces one nitrogen-attached hydrogen atom in these residues with a chlorine atom using the following bond geometries and partial charges: Charge of the chlorine atom: 0.07, charge of the nitrogen atom: -0.61 (based on values for CH_3NHCl (Heeb et al., 2017)), radius of the chlorine atom 1.75 Å (Bondi, 1964), length of the N-Cl bond: 1.784 Å (based on values for NH_2Cl (Harmony et al., 1979)). The resulting manipulated PQR file was then used to calculate the electrostatic surface potential of $RidA_{HOCl}$ using the APBS plugin of PyMol.

The structure of RidA variant R0K0_R105 was modeled using the mutagenesis function of PyMOL. The specified amino acids in wild-type RidA were exchanged as follows:

K3 → T3

K38 → A38

R51 → H51

K58 → G58

K67 → S67

K73 → S73

K79 → T79

R112 → A112

K115 → L115

K118 → L118

R127 → L127

R128 → G128

The electrostatic surface potential for this variant was then calculated as outlined for the wildtype above (conversion of the pdb-file to a PQR file using the PDB2PQR webserver under an assumed pH of 7.0, using PROPKA to assign protonation and the AMBER forcefield and subsequent use of the ABPS plugin in PyMol).

CONFLICT OF INTEREST

The authors declare no conflict of interest.

ACKNOWLEDGMENTS

LIL acknowledges funding from the DFG Priority Program 1710 “Dynamics of Thiol-based Redox Switches in Cellular Physiology” through grant LE2905/1-2. LIL, EH, and JEB would like to thank the DFG Research Training Grant 2341 “Microbial Substrate Conversion” for supporting this work, and JEB further acknowledges funding from the DFG CRC1316-1 and BA 4193/7-1.

AUTHOR CONTRIBUTIONS

MV, JF, AM, LIL conceived and designed the study. NL assisted in and performed protein expression and purification experiments. MV performed mass spectrometry and fluorescence spectroscopy experiments and evaluated MS data. MV and LIL synthesized and characterized the $DANSO_2H$ probe. YS and KSC designed and assisted in the synthesis of the $DANSO_2H$ probe. JF designed and performed site directed mutagenesis experiments, mass spectrometry experiments, and citrate synthase aggregation assays. AM designed site directed mutagenesis experiments and the K0R0_R105 variant and performed citrate synthase aggregation assays. KR and BS performed mass spectrometry measurements and assisted in MS data handling. MK, CJ, TJ, EH, JEB consulted on the computational structure prediction and calculation of the electrostatic surface potential of RidA, $RidA_{HOCl}$ and K0R0_R105. LIL and MV calculated the electrostatic surface potentials. MV, AM, JF, LIL wrote the manuscript, all other authors consulted on the manuscript.

649 REFERENCES

650 **Albrich, J. M., McCarthy, C. A. and Hurst, J. K.** (1981). Biological reactivity of hypochlorous acid:
651 Implications for microbicidal mechanisms of leukocyte myeloperoxidase. *Proceedings of the*
652 *National Academy of Sciences of the United States of America* **78**, 210–214. doi:
653 10.1073/pnas.78.1.210.

654 **Alpmann, A. and Morlock, G.** (2008). Rapid and sensitive determination of acrylamide in drinking
655 water by planar chromatography and fluorescence detection after derivatization with dansulfinic
656 acid. *Journal of Separation Science* **31**, 71–77. doi: 10.1002/jssc.200700391.

657 **Altschul, S. F., Gish, W., Miller, W., Myers, E. W. and Lipman, D. J.** (1990). Basic local alignment
658 search tool. *Journal of Molecular Biology* **215**, 403–410. doi: 10.1016/S0022-2836(05)80360-2.

659 **Ashby, L. V., Springer, R., Hampton, M. B., Kettle, A. J. and Winterbourn, C. C.** (2020).
660 Evaluating the bactericidal action of hypochlorous acid in culture media. *Free Radical Biology*
661 *and Medicine* **159**, 119–124. doi: 10.1016/j.freeradbiomed.2020.07.033.

662 **Bateman, A., Martin, M. J., Orchard, S., Magrane, M., Agivetova, R., Ahmad, S., Alpi, E.,**
663 **Bowler-Barnett, E. H., Britto, R., Bursteinas, B., Bye-A-Jee, H., Coetzee, R., Cukura, A.,**
664 **Silva, A. Da, Denny, P., Dogan, T., Ebenezer, T. G., Fan, J., Castro, L. G., Garmiri, P.,**
665 **Georghiou, G., Gonzales, L., Hatton-Ellis, E., Hussein, A., Ignatchenko, A., Insana, G.,**
666 **Ishtiaq, R., Jokinen, P., Joshi, V., Jyothi, D., Lock, A., Lopez, R., Luciani, A., Luo, J., Lussi,**
667 **Y., MacDougall, A., Madeira, F., Mahmoudy, M., Menchi, M., Mishra, A., Moulang, K.,**
668 **Nightingale, A., Oliveira, C. S., Pundir, S., Qi, G., Raj, S., Rice, D., Lopez, M. R., Saidi, R.,**
669 **Sampson, J., Sawford, T., Speretta, E., Turner, E., Tyagi, N., Vasudev, P., Volynkin, V.,**
670 **Warner, K., Watkins, X., Zaru, R., Zellner, H., Bridge, A., Poux, S., Redaschi, N., Aimo, L.,**
671 **Argoud-Puy, G., Auchincloss, A., Axelsen, K., Bansal, P., Baratin, D., Blatter, M. C.,**
672 **Bolleman, J., Boutet, E., Breuza, L., Casals-Casas, C., de Castro, E., Echioukh, K. C.,**

673 **Coudert, E., Cuche, B., Doche, M., Dornevil, D., Estreicher, A., Famiglietti, M. L.,**
674 **Feuermann, M., Gasteiger, E., Gehant, S., Gerritsen, V., Gos, A., Gruaz-Gumowski, N.,**
675 **Hinz, U., Hulo, C., Hyka-Nouspikel, N., Jungo, F., Keller, G., Kerhornou, A., Lara, V., Le**
676 **Mercier, P., Lieberherr, D., Lombardot, T., et al.** (2021). UniProt: The universal protein
677 knowledgebase in 2021. *Nucleic Acids Research* **49**, D480–D489. doi: 10.1093/nar/gkaa1100.
678 **Bondi, A.** (1964). Van der waals volumes and radii. *Journal of Physical Chemistry* **68**, 441–451. doi:
679 10.1021/j100785a001.
680 **Carr, A. C., Van Den Berg, J. J. M. and Winterbourn, C. C.** (1996). Chlorination of cholesterol in
681 cell membranes by hypochlorous acid. *Archives of Biochemistry and Biophysics* **332**, 63–69. doi:
682 10.1006/abbi.1996.0317.
683 **Cox, J. and Mann, M.** (2008). MaxQuant enables high peptide identification rates, individualized
684 p.p.b.-range mass accuracies and proteome-wide protein quantification. *Nature Biotechnology* **26**,
685 1367–1372. doi: 10.1038/nbt.1511.
686 **Deborde, M. and von Gunten, U.** (2008). Reactions of chlorine with inorganic and organic
687 compounds during water treatment-Kinetics and mechanisms: A critical review. *Water Research*
688 **42**, 13–51. doi: 10.1016/j.watres.2007.07.025.
689 **Goemans, C. V., Vertommen, D., Agrebi, R. and Collet, J. F.** (2018). CnoX Is a Chaperedoxin: A
690 Holdase that Protects Its Substrates from Irreversible Oxidation. *Molecular Cell* **70**, 614–627. doi:
691 10.1016/j.molcel.2018.04.002.
692 **Graf, P. C. F., Martinez-Yamout, M., VanHaerents, S., Lilie, H., Dyson, H. J. and Jakob, U.**
693 (2004). Activation of the Redox-regulated Chaperone Hsp33 by Domain Unfolding. *Journal of*
694 *Biological Chemistry* **279**, 20529–20538. doi: 10.1074/jbc.M401764200.
695 **Gray, W. R.** (1967). [12] Dansyl chloride procedure. *Methods in Enzymology* **11**, 139–151. doi:
696 10.1016/S0076-6879(67)11014-8.

Harmony, M. D., Laurie, V. W., Kuczkowski, R. L., Schwendeman, R. H., Ramsay, D. A., Lovas, F. J., Lafferty, W. J. and Maki, A. G. (1979). Molecular structures of gas phase polyatomic molecules determined by spectroscopic methods. *Journal of Physical and Chemical Reference Data* **8**, 619–722. doi: 10.1063/1.555605.

Hawkins, C. L. and Davies, M. J. (1999). Hygochlorite-induced oxidation of proteins in plasma: Formation of chloramines and nitrogen-centred radicals and their role in protein fragmentation. *Biochemical Journal* **340**, 539–548. doi: 10.1042/0264-6021:3400539.

Hawkins, C. L., Pattison, D. I. and Davies, M. J. (2003). Hypochlorite-induced oxidation of amino acids, peptides and proteins. *Amino Acids* **25**, 259–274. doi: 10.1007/s00726-003-0016-x.

Heeb, M. B., Kristiana, I., Trogolo, D., Arey, J. S. and von Gunten, U. (2017). Formation and reactivity of inorganic and organic chloramines and bromamines during oxidative water treatment. *Water Research* **110**, 91–101. doi: 10.1016/j.watres.2016.11.065.

Hendrikje Buss, I., Senthilmohan, R., Darlow, B. A., Mogridge, N., Kettle, A. J. and Winterbourn, C. C. (2003). 3-Chlorotyrosine as a marker of protein damage by myeloperoxidase in tracheal aspirates from preterm infants: Association with adverse respiratory outcome. *Pediatric Research* **53**, 455–462. doi: 10.1203/01.PDR.0000050655.25689.CE.

Hsieh, W. T. and Matthews, K. S. (1985). Lactose Repressor Protein Modified with Dansyl Chloride: Activity Effects and Fluorescence Properties. *Biochemistry* **24**, 3043–3049. doi: 10.1021/bi00333a036.

Jakob, U., Muse, W., Eser, M. and Bardwell, J. C. A. (1999). Chaperone activity with a redox switch. *Cell* **96**, 341–352. doi: 10.1016/S0092-8674(00)80547-4.

Jersey, J. A., Choshen, E., Jensen, J. N., Johnson, J. D. and Scully, F. E. (1990). N-Chloramine Derivatization Mechanism with Dansyisulfinic Acid: Yields and Routes of Reaction. *Environmental Science and Technology* **24**, 1536–1541. doi: 10.1021/es00080a013.

Jurrus, E., Engel, D., Star, K., Monson, K., Brandi, J., Felberg, L. E., Brookes, D. H., Wilson, L., Chen, J., Liles, K., Chun, M., Li, P., Gohara, D. W., Dolinsky, T., Konecny, R., Koes, D. R., Nielsen, J. E., Head-Gordon, T., Geng, W., Krasny, R., Wei, G. W., Holst, M. J., McCammon, J. A. and Baker, N. A. (2018). Improvements to the APBS biomolecular solvation software suite. *Protein Science* **27**, 112–128. doi: 10.1002/pro.3280.

Käll, L., Storey, J. D., MacCoss, M. J. and Noble, W. S. (2008). Posterior error probabilities and false discovery rates: Two sides of the same coin. *Journal of Proteome Research* **7**, 40–44. doi: 10.1021/pr700739d.

Koldewey, P., Stull, F., Horowitz, S., Martin, R. and Correspondence, J. C. A. B. (2016). Forces Driving Chaperone Action In Brief. *Cell* **166**, 369–379. doi: 10.1016/j.cell.2016.05.054.

Koldewey, P., Horowitz, S. and Bardwell, J. C. A. (2017). Chaperone-client interactions: Non-specificity engenders multifunctionality. *Journal of Biological Chemistry* **292**, 12010–12017. doi: 10.1074/jbc.R117.796862.

Kumar, M. S., Kapoor, M., Sinha, S. and Reddy, G. B. (2005). Insights into hydrophobicity and the chaperone-like function of αA- and αB-crystallins: An isothermal titration calorimetric study. *Journal of Biological Chemistry* **280**, 21726–21730. doi: 10.1074/jbc.M500405200.

Lambrecht, J. A., Flynn, J. M. and Downs, D. M. (2012). Conserved Yjgf protein family deaminates reactive enamine/imine intermediates of pyridoxal 5′-phosphate (PLP)-dependent enzyme reactions. *Journal of Biological Chemistry* **287**, 3454–3461. doi: 10.1074/jbc.M111.304477.

Liu, X., Zeng, J., Chen, X. and Xie, W. (2016). Crystal structures of RidA, an important enzyme for the prevention of toxic side products. *Scientific Reports* **6**,. doi: 10.1038/srep30494.

Mayer, M. P. and Bukau, B. (2005). Hsp70 chaperones: Cellular functions and molecular mechanism. *Cellular and Molecular Life Sciences* **62**, 670–684. doi: 10.1007/s00018-004-4464-6.

McGowan, S. E. and Thompson, R. J. (1989). Extracellular matrix proteoglycan degradation by

human alveolar macrophages and neutrophils. *Journal of Applied Physiology* **66**, 400–409. doi: 10.1152/jappl.1989.66.1.400.

Mortaz, E., Alipoor, S. D., Adcock, I. M., Mumby, S. and Koenderman, L. (2018). Update on neutrophil function in severe inflammation. *Frontiers in Immunology* **9**, 2171. doi: 10.3389/fimmu.2018.02171.

Müller, A., Langklotz, S., Lupilova, N., Kuhlmann, K., Bandow, J. E. and Leichert, L. I. O. (2014). Activation of RidA chaperone function by N-chlorination. *Nature Communications* **5**, 5804. doi: 10.1038/ncomms6804.

Nybo, T., Cai, H., Chuang, C. Y., Gamon, L. F., Rogowska-Wrzesinska, A. and Davies, M. J. (2018). Chlorination and oxidation of human plasma fibronectin by myeloperoxidase-derived oxidants, and its consequences for smooth muscle cell function. *Redox Biology* **19**, 388–400. doi: 10.1016/j.redox.2018.09.005.

Pattison, D. I. and Davies, M. J. (2001). Absolute rate constants for the reaction of hypochlorous acid with protein side chains and peptide bonds. *Chemical Research in Toxicology* **14**, 1453–1464. doi: 10.1021/tx0155451.

Pattison, D. I. and Davies, M. J. (2005). Kinetic analysis of the role of histidine chloramines in hypochlorous acid mediated protein oxidation. *Biochemistry* **44**, 7378–7387. doi: 10.1021/bi0474665.

Pattison, D. and Davies, M. (2006). Reactions of Myeloperoxidase-Derived Oxidants with Biological Substrates:Gaining Chemical Insight into Human Inflammatory Diseases. *Current Medicinal Chemistry* **13**, 3271–3290. doi: 10.2174/092986706778773095.

Pattison, D. I., Davies, M. J. and Hawkins, C. L. (2012). Reactions and reactivity of myeloperoxidase-derived oxidants: Differential biological effects of hypochlorous and hypothiocyanous acids. *Free Radical Research* **46**, 975–995. doi:

10.3109/10715762.2012.667566.

Peskin, A. V and Winterbourn, C. C. (2001). Kinetics of the reactions of hypochlorous acid and amino acid chloramines with thiols, methionine, and ascorbate. *Free Radical Biology and Medicine* **30**, 572–579. doi: 10.1016/S0891-5849(00)00506-2.

Peskin, A. V., Dickerhof, N., Poynton, R. A., Paton, L. N., Pace, P. E., Hampton, M. B. and Winterbourn, C. C. (2013). Hyperoxidation of peroxiredoxins 2 and 3: Rate constants for the reactions of the sulfenic acid of the peroxidatic cysteine. *Journal of Biological Chemistry* **288**, 14170–14177. doi: 10.1074/jbc.M113.460881.

Prütz, W. A. (1996). Hypochlorous acid interactions with thiols, nucleotides, DNA, and other biological substrates. *Archives of Biochemistry and Biophysics* **332**, 110–120. doi: 10.1006/abbi.1996.0322.

Scully, F. E., Yang, J. P., Mazlna, K. and Bernard Daniel, F. (1984). Derivatization of Organic and Inorganic N-Chloramines for High-Performance Liquid Chromatographic Analysis of Chlorinated Water. *Environmental Science and Technology* **18**, 787–792. doi: 10.1021/es00128a012.

Scully, F. E., Mazina, K., Sonenshine, D. and Kopfler, F. (1986). Quantitation and identification of organic N-chloramines formed in stomach fluid on ingestion of aqueous hypochlorite. *Environmental Health Perspectives* **Vol. 69**, 259–265. doi: 10.2307/3430395.

Storz, G., Tartaglia, L. A. and Ames, B. N. (1990). Transcriptional regulator of oxidative stress-inducible genes: Direct activation by oxidation. *Science* **248**, 189–194. doi: 10.1126/science.2183352.

Ulfig, A., Schulz, A. V., Müller, A., Lupilov, N. and Leichert, L. I. (2019). N-chlorination mediates protective and immunomodulatory effects of oxidized human plasma proteins. *eLife* **8**,. doi: 10.7554/eLife.47395.

Ulfig, A., Bader, V., Varatnitskaya, M., Lupilov, N., Winklhofer, K. F. and Leichert, L. I. (2021).

Hypochlorous acid-modified human serum albumin suppresses MHC class II - dependent antigen presentation in pro-inflammatory macrophages. *Redox Biol* **43**:101981. doi: 10.1016/j.redox.2021.101981.

Volz, K. (2008). A test case for structure-based functional assignment: The 1.2 Å crystal structure of the yjgF gene product from Escherichia coli. *Protein Science* **8**, 2428–2437. doi: 10.1110/ps.8.11.2428.

Winter, J., Ilbert, M., Graf, P. C. F., Özcelik, D. and Jakob, U. (2008). Bleach Activates a Redox-Regulated Chaperone by Oxidative Protein Unfolding. *Cell* **135**, 691–701. doi: 10.1016/j.cell.2008.09.024.

Winterbourn, C. C. and Kettle, A. J. (2000). Biomarkers of myeloperoxidase-derived hypochlorous acid. *Free Radical Biology and Medicine* **29**, 403–409. doi: 10.1016/S0891-5849(00)00204-5.

Winterbourn, C. C., van den Berg, J. J. M., Roitman, E. and Kuypers, F. A. (1992). Chlorohydrin formation from unsaturated fatty acids reacted with hypochlorous acid. *Archives of Biochemistry and Biophysics* **296**, 547–555. doi: 10.1016/0003-9861(92)90609-Z.

Winterbourn, C. C., Kettle, A. J. and Hampton, M. B. (2016). Reactive Oxygen Species and Neutrophil Function. *Annual Review of Biochemistry* **85**, 765–792. doi: 10.1146/annurev-biochem-060815-014442.

Zheng, M., Åslund, F. and Storz, G. (1998). Activation of the OxyR transcription factor by reversible disulfide bond formation. *Science* **279**, 1718–1721. doi: 10.1126/science.279.5357.1718.

SUPPLEMENTAL MATERIAL

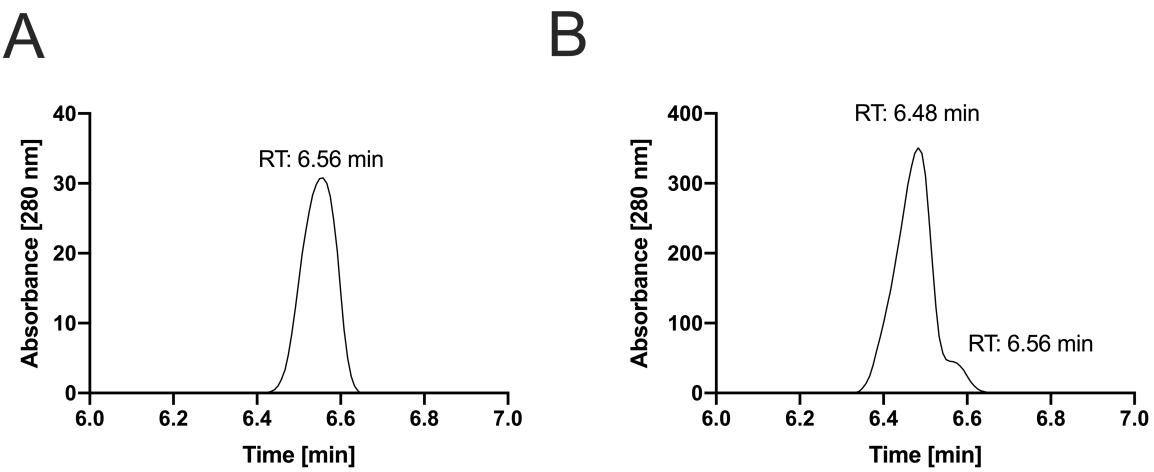

Figure S1. High-performance liquid chromatography (HPLC) of $DANSO_3H$ and $DANSO_2H$ (A) HPLC measurement of 10 µM dansyl sulfonic acid ($DANSO_3H$). The absorbance A_{280} reached its maximum at 6.56 min. **(B)** HPLC of 100 µM dansyl sulfinic acid ($DANSO_2H$). Two absorbance peaks could be distinguished: at 6.48 min, corresponding presumably to $DANSO_2H$ and a lower peak at 6.56 min corresponding to the contamination with $DANSO_3H$, as determined using $DANSO_3H$-standard.

Suppelemental Material S2: Python script for the manipulation of PQR-files to generate a predicted structure for RidAHOCl from PDB structure 1qu9.

```
# Enter all the user input you need and run as
# % python3 Convert_pqr_to_HOCl_pqr_R105.py > outputfilename.pqrfile
#
# The parser is not super robust. It expects a very specific type of pqr file. To get the
# chain you need to use the “Add/keep chain IDs in the PQR file option” of PDB2PQR
# The format is:
# 0:Field_name
# 1:Atom_number
# 2:Atom_name
# 3:Residue_name
# 4:Chain
# 5:Residue_number
# 6:X
# 7:Y
# 8:Z
# 9:Charge
# 10:Radius
# Furthermore, it just prepends an X to any line that should be removed and it does
# not change residue numbering. Luckily, PyMOL figures it out just fine and when you
# File > Export Molecule... and save as pqr, it formats everything nicely...

################################################################################

 #     #  #####  ####### ######     ### #     # ######  #     # #######
 #     # #     # #       #     #     #  ##    # #     # #     #    #
 #     # #       #       #     #     #  # #   # #     # #     #    #
 #     #  #####  #####   ######      #  #  #  # ######  #     #    #
 #     #       # #       #   #       #  #   # # #       #     #    #
 #     # #     # #       #    #      #  #    ## #       #     #    #
  #####   #####  ####### #     #    ### #     # #        #####     #

################################################################################

# Enter the name of the pqr file you want to modify here. This file should be in the same
# directory you are running your script from (or you need to provide a path).

pqrfile = open("RidA_1qu9.pqr", 'r')

# Parameters for Lysine

ClZLys_charge = "0.0700" #according to: Heeb et al. 2017 Water research, table 2 (doi:10.1016/j.watres.2016.11.065) in electrons
ClZLys_radius = "1.7500" #according to: Bondi 1964 (doi:10.1021/j100785a001) van der Waals radius, in Å
NZLys_charge = "-0.6100" #according to: Heeb et al. 2017 Water research, table 2 (doi:10.1016/j.watres.2016.11.065) in electrons
NClLys_bondlength = 1.748 #according to: Harmony et al. 1979, data for NH2Cl, (doi:10.1063/1.555605) in Å

# Parameters for Arginine

ClH2Arg_charge = "0.0700" #same as above
ClH2Arg_radius = "1.7500" #same as above
NH2Arg_charge = "-0.6100" #same as above
NClArg_bondlength = 1.748 #same as above
NHArg_bondlength = 1 #good guess

# Here you can enter residues to exclude as an array just so:
# residue_to_exclude = ["3", "105", "128"] for Lysine K3 and Arginines R105 and R128
residue_to_exclude = ["105"]
```

```
################################################################################

  #####   #####  ######  ### ######  #######     #####  #######    #    ######  ######  #####
 #     # #     # #     #  #  #     #    #       #     #    #      # #   #     #    #    #     #
 #       #       #     #  #  #     #    #       #          #     #   #  #     #    #    #
  #####  #       ######   #  ######    #        #####     #    #     # ######    #     #####
       # #       #   #    #  #         #             #    #    ####### #   #     #          #
 #     # #     # #    #   #  #         #       #     #    #    #     # #    #    #    #     #
  #####   #####  #     # ### #         #        #####     #    #     # #     #   #     #####

################################################################################

for line in pqrfile:
    mystring = line
    row = mystring.split()
#    print (row)
#    print ('my array has ', len(row), 'elements')
    if row[0] == "ATOM":

################################################################################

 #       #     #  #####  ### #     # #######         |        This part of the script
 #        #   #  #     #  #  ##    # #               |        modifies all the lysine
 #         # #   #        #  # #   # #               |        residues.
 #          #    #####   #  #  #  # #####       \   |  /
 #          #          #  #  #   # # #            \  | /
 #          #    #     #  #  #    ## #             \|/
 #######    #     #####  ### #     # #######         v

################################################################################

        if row[3] == "LYS":
            if row[5] in residue_to_exclude:
                print (mystring, end = "")
            elif row[2] == "NZ":
#                print ("!NZ", end = " ")
                xNZ = float(row[6]) #remember those X, Y, Z coordinates to calculate the correct bond length later
                yNZ = float(row[7])
                zNZ = float(row[8])
                print (row[0], " ", row[1], " ", row[2], " ", row[3], " ", row[4], " ", row[5], " ", row[6], " ", row[7], " ", row[8], " ", NZLys_charge, " ",
row[10])
            elif row[2] == "HZ1":
#                print ("!HZ1", end = " ")
                print (row[0], " ", row[1], " ", "HZ", " ", row[3], " ", row[4], " ", row[5], " ", row[6], " ", row[7], " ", row[8], " ", row[9], " ", row[10])
            elif row[2] == "HZ2":
#                print ("!HZ2", end = " ")
                xHZ2 = float(row[6]) #I also need those X, Y, Z coordinates to calculate the correct bond length
                yHZ2 = float(row[7])
                zHZ2 = float(row[8])
                # Calculate bond length (or rather the correct XYZ coordinates for ClZ)
                # This is a complicated one. Here I first need to define the line equation in the form
                #
                # x(ClZ) = x(NZ) + (x(NZ)-x(HZ2))*t
                # x(ClZ) = x(NZ) + (x(NZ)-x(HZ2))*t
                # x(ClZ) = x(NZ) + (x(NZ)-x(HZ2))*t
                #
                # Now I have to find t. This I do with an equation that I painstakingly calculated on a sheet of (word-)paper.
                t = -(((NClLys_bondlength**2)/((xNZ - xHZ2)**2 + (yNZ - yHZ2)**2 + (zNZ - zHZ2)**2))**0.5)
#                print ("t is ", t)
                #now for the calculation of the new X,Y,Z values
                xClZ = round((xNZ + ((xNZ-xHZ2)*t)), 3)
                yClZ = round((yNZ + ((yNZ-yHZ2)*t)), 3)
                zClZ = round((zNZ + ((zNZ-zHZ2)*t)), 3)
#                print ("xNZ: ", xNZ, "xHZ2: ", xHZ2, "xClZ: ", xClZ)
#                print ("yNZ: ", yNZ, "yHZ2: ", yHZ2, "yClZ: ", yClZ)
#                print ("zNZ: ", zNZ, "zHZ2: ", zHZ2, "zClZ: ", zClZ)
#                And now a calculation of the distance
#                distance = ((xNZ - xClZ)**2 + (yNZ - yClZ)**2 + (zNZ - zClZ)**2)**0.5
#                print ("And the distance is : ", distance)
                print (row[0], " ", row[1], " ", "ClZ", " ", row[3], " ", row[4], " ", row[5], " ", xClZ, " ", yClZ, " ", zClZ, " ", ClZLys_charge, " ",
ClZLys_radius)
            elif row[2] == "HZ3":
#                print ("!HZ3", end = " ")
                print ("X ", mystring, end = "")
            else:
                print (mystring, end = "")

################################################################################

    #    ######   #####  ### #     # ### #     # #######         |        This part of the
   # #   #     # #     #  #  ##    #  #  ##    # #               |        script modifies
  #   #  #     # #        #  # #   #  #  # #   # #               |        all arginine
 #     # ######  #  #### #  #  #  #  #  #  #  # #####       \   |  /     residues.
 ####### #   #   #     #  #  #   # #  #  #   # #            \  | /
 #     # #    #  #     #  #  #    ##  #  #    ## #             \|/
 #     # #     #  #####  ### #     # ### #     # #######         v

################################################################################

        elif row[3] == "ARG":
            if row[5] in residue_to_exclude:
                print (mystring, end = "")
            elif row[2] == "CZ":
                xCZ = float(row[6]) #remember those X, Y, Z coordinates to straighten out the bond from NH1 to only one hydrogen
                yCZ = float(row[7])
                zCZ = float(row[8])
                print (mystring, end = "")
            elif row[2] == "NH1":
                xNH1 = float(row[6]) #remember those X, Y, Z coordinates, too, to straighten out the bond from NH1 to only one hydrogen
                yNH1 = float(row[7])
                zNH1 = float(row[8])
                print (mystring, end = "")
            elif  row[2] == "NH2":
                xNH2 = float(row[6]) #remember those X, Y, Z coordinates to calculate the correct NCl bondlength
                yNH2 = float(row[7])
                zNH2 = float(row[8])
                print (row[0], " ", row[1], " ", row[2], " ", row[3], " ", row[4], " ", row[5], " ", row[6], " ", row[7], " ", row[8], " ", NH2Arg_charge, " ",
row[10])
            elif row[2] == "HH11":
                print ("X ", mystring, end = "") #remove this H
            elif row[2] == "HH12":
                #straighten this guy out. Do it by putting the now single H on the line made by NH1 and CZ
                #similar to above. First calculate the t (this time with a different sign, the H atom is in the other direction and not replacing one of those atoms)
                t = ((NHArg_bondlength**2)/((xNH1 - xCZ)**2 + (yNH1 - yCZ)**2 + (zNH1 - zCZ)**2))**0.5
                #then use the t to calculate the new coordinates for the single H
                xHH1 = round((xNH1 + ((xNH1-xCZ)*t)), 3)
                yHH1 = round((yNH1 + ((yNH1-yCZ)*t)), 3)
                zHH1 = round((zNH1 + ((zNH1-zCZ)*t)), 3)
#                And now a calculation of the distance
#                distance = ((xHH1 - xNH1)**2 + (yHH1 - yNH1)**2 + (zHH1 - zNH1)**2)**0.5
#                print ("And the distance is : ", distance)
```

```
                print (row[0], " ", row[1], " ", "HH1", " ", row[3], " ", row[4], " ", row[5], " ", xHH1, " ", yHH1, " ", zHH1, " ", row[9], " ", row[10])
            elif row[2] == "HH21":
                #this gal needs to be replaced with the Cl. So again we need to calculate the correct XYZ position.
                #for this we need the original position
                xHH21 = float(row[6]) #I also need those X, Y, Z coordinates to calculate the correct bond length
                yHH21 = float(row[7])
                zHH21 = float(row[8])
                #then we calculate t
                t = -(((NClArg_bondlength**2)/((xNH2 - xHH21)**2 + (yNH2 - yHH21)**2 + (zNH2 - zHH21)**2))**0.5)
                #now for the calculation of the new X,Y,Z values
                xClH2 = round((xNH2 + ((xNH2-xHH21)*t)), 3)
                yClH2 = round((yNH2 + ((yNH2-yHH21)*t)), 3)
                zClH2 = round((zNH2 + ((zNH2-zHH21)*t)), 3)
#                And now a calculation of the distance
#                distance = ((xNH2 - xClH2)**2 + (yNH2 - yClH2)**2 + (zNH2 - zClH2)**2)**0.5
#                print ("And the distance is : ", distance)
                print (row[0], " ", row[1], " ", "ClH2", " ", row[3], " ", row[4], " ", row[5], " ", xClH2, " ", yClH2, " ", zClH2, " ", ClH2Arg_charge, " ",
ClH2Arg_radius)
            else:
                print (mystring, end = "")

################################################################################

    #    #      #         ####### ####### #     # ####### ######       #      #
   # #   #      #         #     #    #    #     # #       #     #     # #    # #
  #   #  #      #         #     #    #    #     # #       #     #    #   #  #   #
 #     # #      #         #     #    #    ####### #####   ######    #     # #     #
 ####### #      #         #     #    #    #     # #       #   #     ####### #######
 #     # #      #         #     #    #    #     # #       #    #    #     # #     #
 #     # ####### #######   #######    #    #     # ####### #     #   #     # #     #

################################################################################

        else:
            print (mystring, end = "")

################################################################################

 #     # ####### #######      #    #     #      #      #
 ##    # #     #    #        # #   ##    #     # #     # #
 # #   # #     #    #       #   #  # #   #    #   #   #   #
 #  #  # #     #    #      #     # #  #   #    #     # #     #
 #   # # #     #    #      ####### #   # #    ####### #######
 #    ## #     #    #      #     # #    ##    #     # #     #
 #     # #######    #      #     # #     #    #     # #     #

################################################################################

    else:
        print (mystring, end = "")
```